ACS OMEGA

http://pubs.acs.org/journal/acsodf

Article

Dereplication Based Strategy for Rapid Identification and Isolation of a Novel Anti-inflammatory Flavonoid by LCMS/MS from *Colebrookea oppositifolia*

Neha Sharma,[¶] Vidushi Khajuria,[¶] Shilpa Gupta, Chetan Kumar, Anjana Sharma, Nazir Ahmad Lone, Satya Paul, Siya Ram Meena, Zabeer Ahmed,* Naresh Kumar Satti,* and Mahendra Kumar Verma*

Cite This: *ACS Omega* 2021, 6, 30241−30259

Read Online

ACCESS | Metrics & More | Article Recommendations | Supporting Information

ABSTRACT: *Colebrookea oppositifolia* is a folkloric medicinal plant, well known for its tremendous medicinal properties such as curing epilepsy, ulcers, and urinary problems. The aim of the present study was to apply the dereplication strategy on the ethanol extract of *C. oppositifolia* with potent anti-inflammatory activity for the rapid identification and isolation of novel bioactive molecules to aid the drug discovery process. An integrated approach using liquid chromatography−mass spectrometry (LCMS) followed by preparative high-performance liquid chromatography (HPLC) was used for the isolation of potent molecules from the anti-inflammatory extract of *C. oppositifolia*. Purity of the compounds (>98.5%) was established by HPLC, and identification was carried out by NMR and ESI-MS. 5,6,7-Trihydroxyflavone-3-*O*-glucuronide methyl ester (compound III) isolated from *C. oppositifolia* was extensively studied for anti-inflammatory potential in lipopolysaccharide (LPS)-stimulated RAW 264.7 cells and the mice model. Compound III significantly repressed various proinflammatory mediators and upregulated the release of anti-inflammatory cytokine IL-10. Compound III reduced inflammation when studied for parameters such as the phagocytic index, carrageenan-induced paw edema in mice, and effect on organ weight. It reduced inflammation in a dose-dependent manner both *in vitro* and *in vivo*. Further molecular insights into the study revealed that compound III blocks the phosphorylation of I kappa b kinase α/β (IKKα/β), IκBα, and nuclear factor kB p65 (NF-κBp65) which is a key controller of inflammation, thereby showing anti-inflammatory potential. Hence, this study permits further investigation to develop compound III as an anti-inflammatory drug.

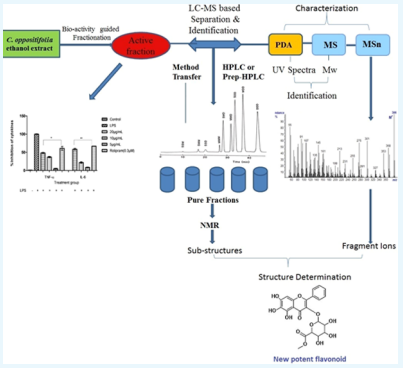

1. INTRODUCTION

Natural products have always been a major source of chemical diversification and drug leads in the pharmaceutical industry. Today, about 60% of antitumor, anticancer, and anti-infective drugs commercially available or in the clinical trials are either pure natural products or inspired by their scaffolds, but the drug-discovery process in the natural products has never been a cakewalk.[1−4] The initial screening of the plant or microbial extracts followed by bioguided fractionation for the isolation of pure compounds from solvents of varied polarities, it is very laborious, resource-intensive, costly, and time-consuming affair which often ends up with the known or trivial molecules in hands.[5−7] Multifaceted approaches are being applied through hyphenated techniques to discover novel lead-like molecules to scuffle various existing detrimental diseases but in a much speedy way rather than following the conventional isolation protocols. Dereplication *via* liquid chromatography−mass spectrometry (LCMS/MS) has been dominating the charts of the latest analytical platforms for *de novo* isolation from the last few years.[8−12]

Dereplication is the process of eliminating the already known and the undesired molecules from the novel candidates in the crude plant or microbial extracts. Mass spectrometry is an ultimate tool which can be employed for the identification of novel candidates in a much shorter time, which is neither cost-effective nor labor-intensive unlike the conventional methods of isolation which often end up with the trivial molecules in hand.[7] The LCMS/MS-based dereplication strategy was employed to a well-known medicinal plant *Colebrookea oppositifolia* (Lamiaceae) commonly known as "Indian squirrel tail" which is a woolly shrub, distributed mostly in subtropical regions of the world such as India, Pakistan, Nepal, Myanmar, Thailand, and Southwest China.[13] It is a folkloric medicinal plant used in treating wounds, bruises, and fractures; for its anti-inflammatory properties.[14−17] Roots of the plants are employed in curing epilepsy, peptic ulcers, and haemostasis and to relieve tonsillitis.[18,19] Shoots of *C. oppositifolia* are used in the treatment of urinary problems,[20]

Received: April 6, 2021
Accepted: August 26, 2021
Published: November 2, 2021

https://doi.org/10.1021/acsomega.1c01837
ACS Omega 2021, 6, 30241−30259

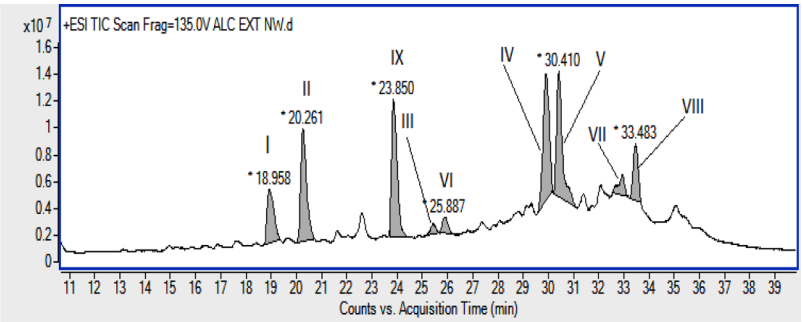

Figure 1. LC-ESI-MS chromatogram of the ethanol extract of *C. oppositifolia*.

Table 1. MS and MS/MS Analysis Results of Different Isolated Compounds

S.No	compound code	retention time (in min)	calculated mass $(M + H)^+$	observed mass $(M + H)^+$	formula generated	ppm error	MS/MS	collision energy used (in volts)
1.	I	18.9	625.2126	625.2132	$C_{29}H_{36}O_{15}$	−0.85	144.10, 182.05,335.08, 498.35, 245.22, 104.10	20
2.	II	20.2	463.0871	463.0864	$C_{21}H_{18}O_{12}$	1.56	390.30, 166.08, 144.10, 254.13, 86.06, 446.32, 404.31	40
3.	III	25.4	477.1027	477.1019	$C_{22}H_{20}O_{12}$	−0.74	390.30, 144.10,254.13, 70.06	40
4.	IV	29.8	313.1070	313.1071	$C_{18}H_{16}O_5$	1.02	283.05, 182.05, 98.05, 255.06, 153.01, 144.10, 269.08, 251.06, 297.07, 223.07, 172.13, 70.06, 81.07	40
5.	V	30.4	343.1176	343.1179	$C_{19}H_{18}O_6$	−0.45	313.06, 285.07, 124.07, 153.01, 181.01, 299.09, 327.08, 256.07, 95.08, 55.05	40
6.	VI	25.1	447.1285	447.1300	$C_{22}H_{22}O_{10}$	−2.98	444.30, 390.30, 144.10, 100.11, 70.06, 166.08, 86.06, 123.11, 210.14, 374.34	40
7.	VII	32.9	329.1019	329.1026	$C_{18}H_{16}O_6$	−1.83	124.07, 313.07, 285.07, 153.01, 299.09, 98.09,327.08	40
8.	VIII	33.4	359.1125	359.1092	$C_{19}H_{18}O_7$	0.33	144.10, 95.08, 81.07, 69.07, 154.08, 283.05, 301.07	40
9.	IX	23.3	447.0921	447.0966	$C_{21}H_{18}O_{11}$	0.3	475.32, 390.30, 144.10, 166.08, 460.34	40

whereas leaf juice relieves fever and headache and juice of the young inflorescence is used to cure sinusitis.[21] Oil of the plant has fungitoxic properties.[22] Wide pharmacological applications of *C. oppositifolia* in the traditional medicines prompted us to carry out the chemical investigation of this species *via* the dereplication approach in the hope of obtaining novel bioactive future drug candidates. To reveal the potential of *C. oppositifolia*, as a part of our ongoing research, initially we assayed the ability of the ethanol extract of *C. oppositifolia* to decrease lipopolysaccharide (LPS)-induced tumor necrosis factor-α (TNF-α) and interleukin-6 (IL-6) production in the murine macrophage RAW 264.7 cell line. Proinflammatory cytokines are crucial mediators in the regulation of immune response and thus contribute to various inflammatory disorders. Several cell types such as macrophages and T cells together with extracellular mediators of the immune system are key components in the regulation of the inflammatory process, TNF-α and IL-6 being the important ones. They act as proinflammatory mediators in a variety of diseases such as pain and joint destruction, rheumatoid arthiritis.[23] Nowadays, a big effort has been made in terms of TNF-α inhibition, but no small molecule has been approved as a reliable inhibitor of this cytokine so far. TNF-α inhibitor drugs such as infliximab, adalimumab, and etanercept in clinics are proteins having undesirable side effects such as infections in the upper respiratory tract, liver function test (LFT) abnormalities, and hepatitis B virus reactivation. IL-6 inhibitors are found to be effective for the treatment of Alzheimer's disease, cancer, psychiatric disorders, diabetes, and depression,[24−31] converting the synthesis and isolation of IL-6 inhibitors into a major hope for the anti-inflammatory drug development. Prostaglandins, eicosanoid lipid mediators, and leukotrienes play a major part in inflammation.[32] Leukotrienes are potent lipid mediators associated with many allergic reactions and secreted in response to cellular activation by immune complexes. They are secreted by inflammatory cells such as polymorphonuclear leukocytes, macrophages, and mast cells. The cellular activation by immune complexes, bacterial peptides, and other stimuli elicit the macrophage response.[33−35] Monocytes/macrophages play a vital role in expression of the resistance molecules to remove foreign or infectious agents and release of inflammatory mediators including TNF-α, IL-6, NO, and prostaglandinE2 (PGE2).[36,37] Extensive expressions of the cytokines and other proinflammatory mediators have direct relationship with the excessive inflammation events and the pathogenesis of chronic diseases.[38] For the inflammatory progression, inducible NO synthase (iNOS) and cyclooxygenase2 (COX-2) are significant regulators and these enzymes when upregulated synthesize enzyme reaction products of NO and PGE2, respectively. iNOS and COX-2 catalyze L-arginine into L-citrulline and synthesize prostaglandins from arachidonic acid, respectively. The two enzymes are believed to be imperative inflammatory mediators.[39,40] The state of inflammation in monocyte/macrophage-stimulated LPS, nuclear factor-κB (NF-κB), and the mitogen-activated protein kinase (MAPK) pathway are triggered. These responses are to react in contradiction of the abnormal cellular shock state. These two pathways induce inflammatory mediators such as NO and PGE2. Generally, the aforesaid two pathways activated by LPS are downstream of the toll-like receptor (TLR) 4 signaling, as are known as the myeloid differentiation factor 88 (MyD88)-dependent pathway and the

https://doi.org/10.1021/acsomega.1c01837
ACS Omega 2021, 6, 30241−30259

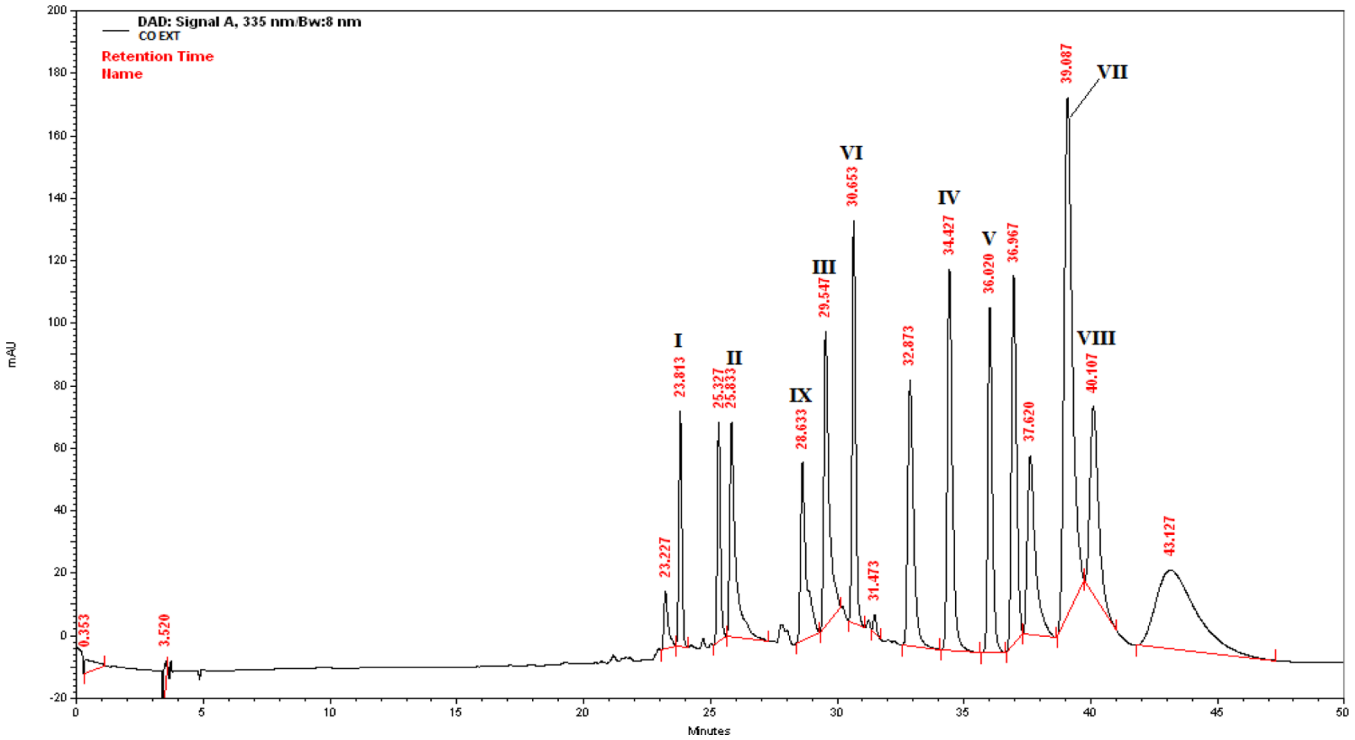

Figure 2. Preparative HPLC chromatogram of the ethanol extract of *C. oppositifolia*.

MyD88-independent pathway. Therefore, MyD88-dependent downstream is composed of the NF-kB and MAPK pathway. It is reported that these two pathways induce inflammatory mediators such as NO and PGE2.[41] It is always necessary to confirm the *in vitro* results in *in vivo* models. Hence, the *in vivo* effect of compound III was also studied in LPS-induced inflammatory mice.[42] Thus, the present investigation aimed to isolate novel drug candidates *via* the LCMS/MS-based dereplication strategy and to investigate their detailed anti-inflammatory potential.

2. RESULTS

2.1. Isolation and Characterization of the Isolated Molecules. Although, in the previous phytochemical investigations, a number of flavones and their glycosides have been reported from the bark, stem, and leaves of this plant,[43−46] we were successful in applying the LCMS/MS-based dereplication approach to identify (Figure 1) new compounds from the ethanol extract of the plant leaves, for which separation was achieved in such a way so that each peak gets separated. This reveals the retention time and molecular weight of each peak. This information helped us to find out whether compounds are known or unknown by searching different available chemical search databases, *viz.*, Scifinder and DNP (dictionary of natural products). Results obtained by tandem mass spectrometry experiments are presented in Table 1.

The method which was used for LCMS/MS was scaled up on preparative high-performance liquid chromatography (HPLC) with certain modifications (Figure 2) for the effective isolation of nine molecules, *viz.*, **I**, acteoside; **II**, 5,7,4′-trihydroxyflavone-3-*O*-glucuronide; **III**, 5,6,7-trihydroxyflavone-3-*O*-glucuronide methyl ester; **IV**, 5,6,7-trimethoxyflavone; **V**, 5,6,7,4′-tetramethoxyflavone; **VI**, 5-hydroxy-7-methoxy-flavone-6-*O*-glucopyranosyl; **VII**, 5-hydroxy-6,7,8-trimethoxy flavone; **VIII**, 5-hydroxy-6,7,8,4′-tetramethoxy flavone; and **IX**, 5,6,7-trihydroxyflavone-7-*O*-glucuronide from the ethanol extract of the plant (Figure 3). Out of the nine isolated molecules, **III** came out to be a new and highly potent anti-inflammatory molecule by both *in vitro* and *in vivo* studies. **II**, **III**, and **IV** have been reported for the first time from this plant. The identity of the isolated molecules was achieved on the basis of NMR and mass spectrometry data and was further confirmed by comparing their spectroscopic data with the ones already reported in the literature.

2.1.1. Structure Elucidation of New Flavonoid, III. Compound **III** was obtained as a dark brown light-weight solid. Analysis of the ^{13}C NMR revealed 20 resonances (Figure 4) with two of them corresponding to two equivalent carbons each, thereby making a total of 22 carbon atoms in the structure which was verified in DEPT-135 spectra exhibiting 10 positive signals, indicating the presence of 10 primary and tertiary carbons and no CH_2 group in the molecule (Figure 5). HR-ESI-MS analysis generated a molecular ion peak $[M + H]^+$ at m/z 477 deducing a molecular formula of $C_{22}H_{20}O_{12}$ (Figure 6). Its IR spectrum showed absorptions corresponding to hydroxyl (3384 cm^{-1}) and carbonyl (1652 cm^{-1}) functionalities in the structure. IR bands in the range of 1015 to 1750 cm^{-1} reflected a typical flavonoid structure, and the absorptions of 3384 and 3584 cm^{-1} indicated the presence of OH groups in the structure (Figure 7). The UV absorptions at 281 and 303 nm supported the presence of benzoyl and the cinnamoyl bands in flavonoid (Figure 8). On the basis of chemical shifts (δ) and integration, the ^{1}H NMR spectrum of compound III (Figure 9) can be summarized as follows: δ (in ppm) 5.97 (s, 1H, H-8), 6.30 (br s, 2H, H-3′ & 5′), 7.06 (d, J = 4.64 Hz, 3H, H-2′, 4′ & 6′), 5.02 (d, J = 4.6 Hz, 1H, H-1″), 3.89 (d, J = 9.4 Hz, 1H, H-2″), 3.6 (m, 2H, H-3″ & 4″), 3.7 (m, 1H, H-5″) and 3.5 (s, 3H, $-OCH_3$).The δ at 5.97 ppm corresponds to an olefinic hydrogen in the A ring, and the signal appeared as a singlet due to the lack of vicinal hydrogen.

https://doi.org/10.1021/acsomega.1c01837
ACS Omega 2021, 6, 30241−30259

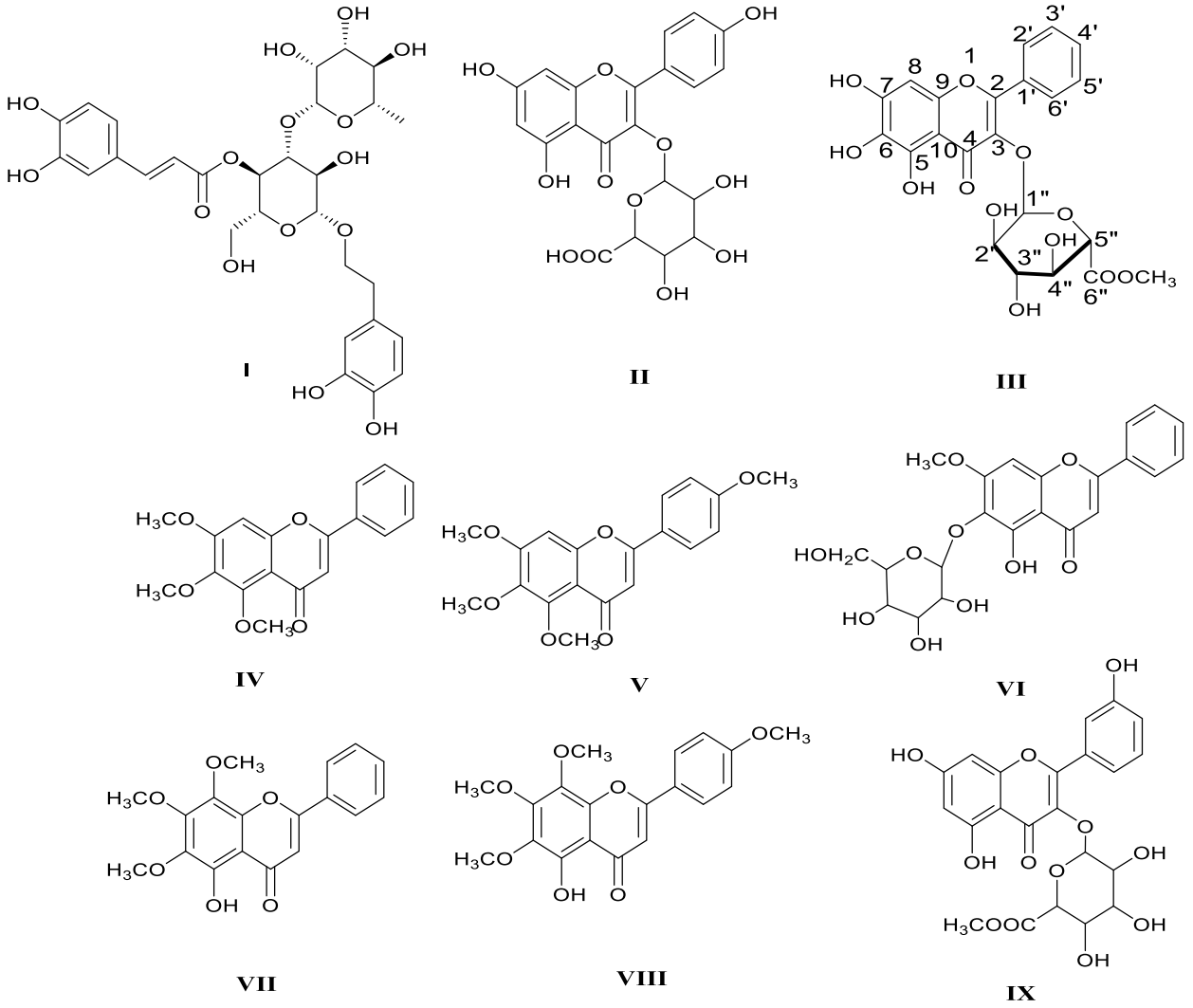

Figure 3. Chemical structures of the compounds isolated from *C. oppositifolia*.

A doublet at 7.06 ppm and a broad singlet at 6.30 ppm accounting for five protons suggested that there is no substitution in the B ring. Two different sets of protons of the B-ring (*i.e.* 2′, 4′, and 6′ and 3′ and 5′) are chemically but not magnetically equivalent; thus, the five protons of the B-ring are behaving somewhat like a five-spin system. The doublet signal centered at 7.06 ppm is characteristic for the aromatic protons on the B-ring at 2′, 4′, and 6′. The electrons on the 6′ proton could be somewhat affected by the neighboring ether oxygen of the C-ring, as a result of which the ortho and meta coupling constants would be slightly different. However, due to the complex nature of the obtained spectra, coupling constants for ortho protons and the meta protons could not be calculated. However, the ^{1}H signals of the aromatic protons at 3′ and 5′ showed a broad singlet, and integration of this broad singlet revealed that there are two protons at the signal centered at δ 6.30 and thus were assigned to the respective positions. A singlet at 5.97, slightly less than the typical H-8 value in the flavonoid pattern, suggested the presence of the hydroxyl group (e^{-} releasing group, leading to the upfield shifting) at the H-7 position. The absence of the typical δ value close to 6.4 and the presence of quaternary carbons suggested the presence of the hydroxyl moiety at H-6. Interpretation of the carbon signals was also supported by the information on 5,7-dihydroxyflavonoids,[47] such as the ^{13}C signal of C−8 in these flavones appears generally in the range of 90 to 100 ppm and the resonance corresponding to C−4 typically appears in the range of 176 to 196 ppm depending upon the type of flavonoid. The presence of a multiplet with the chemical shift range of 3.6 ppm corresponded to two protons of the glucuronide at H-3″ and H-4″ positions along with a multiplet at 3.7 ppm for H-5″ including a methoxy group reflecting the carbon of the $-OCH_3$ in the glucuronide with a clear singlet at 3.5 ppm. Glucuronide is an α anomer with protons of the anomeric carbon showing resonance at 5.02 ppm with a coupling constant of 4.6 Hz and its corresponding carbon at 100.1 ppm which are the characteristics for the α anomer. It is evident from the NOE among H-1″, H-2″, and H-4″ and between H-3″ and H-5″, which also clearly indicates the presence of the α anomer of glucuronide.

A doublet with a coupling constant of 9.4 Hz at δ 3.89 was assigned to H-2″ of the glucuronide. The structure was further confirmed on the basis of 2D NMR experiments (Table 2 and Figure 10).

Heteronuclear multiple-bond coherence experiments were also performed. The HMBC correlations (Figures 11 and 12) were observed from H-8 (δ 5.97) to C-2 (δ 163.7) and C-10 (δ 105.1), H-6′ (δ 7.06) and H-3″ (δ 3.6) to C-3 (δ 161.6), H-

https://doi.org/10.1021/acsomega.1c01837
ACS Omega 2021, 6, 30241−30259

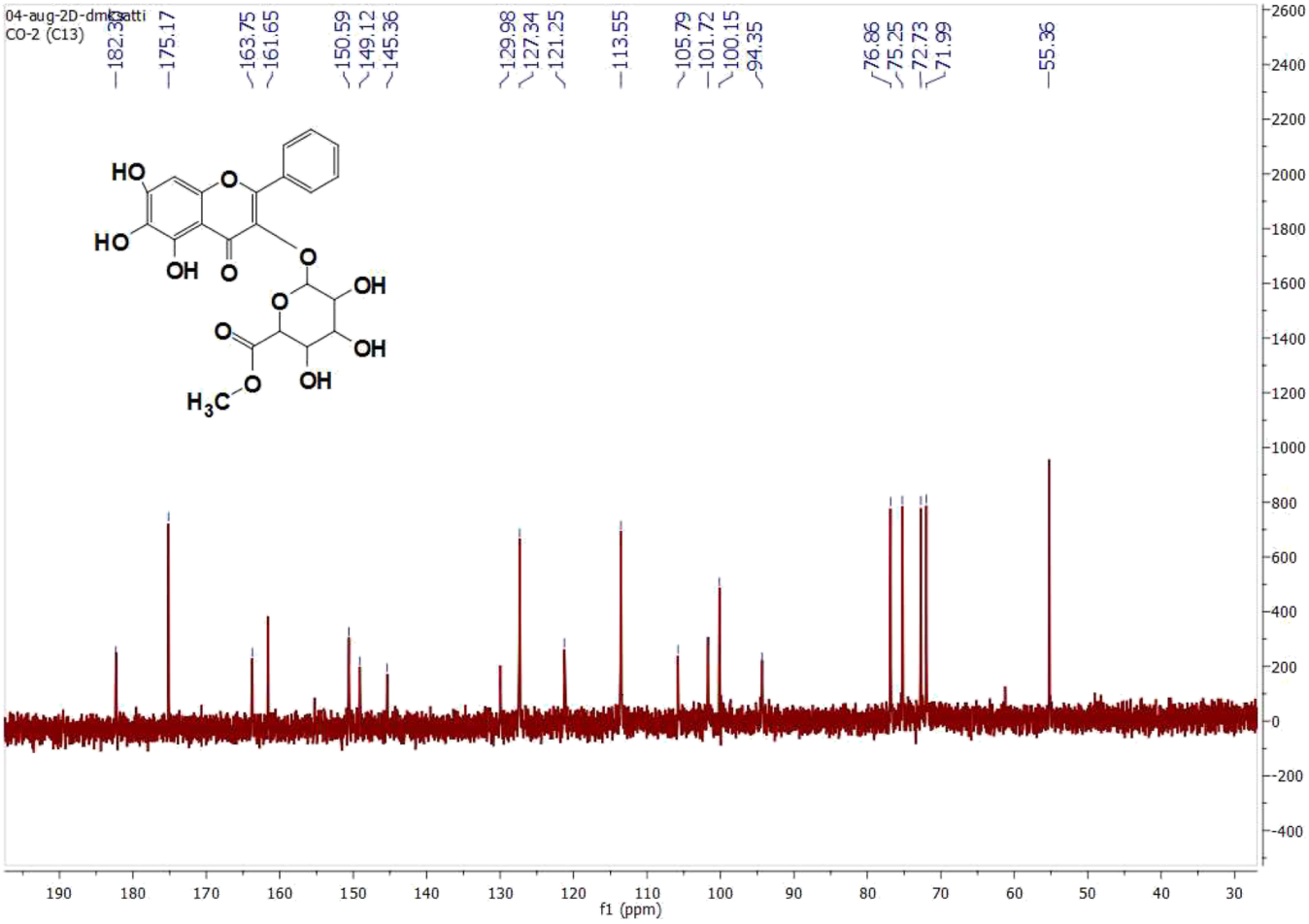

Figure 4. ^{13}C NMR spectra of **III**.

2″ (δ 3.89) to C-4 (δ 182.3), H-3′/H-5′ (δ 6.3) to C-1′ (δ 129.9), H-3″ and H-4″ (δ 3.6) to C-1″ (δ 100.1), H-2″ (δ 3.89), H-5″ (δ 3.7) to C-3″ (δ 71.9), H-3″ (δ 3.6) to C-5″ (δ 75.2), and H-3″, H-4″ (δ 3.6) to C-6″ (δ 175.1)

2.1.2. Spectral Data of the Isolated Molecules. 2.1.2.1. Compound-I. Yellow crystal from ethyl acetate; melting point 143−146 °C; (+) HR-ESI-MS observed at m/z 625.21 $(M + H)^+$, calculated for $C_{29}H_{38}O_{15}$, 624.21. ^{1}H NMR (400 MHz, CD_3OD): δ ppm: 0.98 (3H, d, J = 6.2 Hz, CH_3 of rhamnose), 2.19 (2H, t, J = 6.6 Hz, Ar−CH_2−), 4.27 (1H, d, J = 7.9 Hz, H-1 of glucose), 5.08 (1H, d, J = 1.2 Hz, H-1 of rhamnose), 6.17 (1H, d, J = 15.8 Hz, Ar−CH═CH−), 7.49 (1H, d, J = 15.8 Hz, Ar−CH═CH−), 6.4−6.9 (6H, aromatic H); ^{13}C NMR (100.61 MHz, CD_3OD) δ ppm: 131.5 (HT-1), 117.1 (HT-2), 146.1 (HT-3), 144.6 (HT-4), 116.3 (HT-5), 121.3 (HT-6), 72.2 (HT-7)*, 36.5 (HT-8)*, 127.7 (Caf-1), 115.3 (Caf-2), 146.8 (Caf-3), 149.8 (Caf-4), 116.5 (Caf-5), 123.2 (Caf-6), 148.0 (Caf-7; γ), 114.7 (Caf-8; β), 168.2 (Caf-9; α), 104.2 (G-1), 76.2 (G-2), 81.6 (G-3), 70.6 (G-4), 76.08 (G-5), 62.4 (G-6), 103.04 (R-1), 72.3 (R-2), 72.1 (R-3), 73.8 (R-4), 70.4 (R-5), 18.4 (R-6).[48]

2.1.2.2. Compound-II. Yellow crystal from ethyl acetate; melting point 189−191 °C; HR-ESI + MS observed at m/z 463.08 $(M + H)^+$, calculated for $C_{21}H_{18}O_{12}$, 462.07. ^{1}H NMR (500 MHz, D_2O): δ ppm: 6.28 (1H, s, H-6), 5.95 (1H, s, H-8), 7.1 (2H, d, J = 0.7 Hz, H-2′, 6′), 6.40 (2H, br s, H-3′, 5′), 4.94 (1H, br d, J = 2.9 Hz, H-1″); ^{13}C NMR (125 MHz, D_2O): δ ppm: 151.9 (s, C-2), 130.81 (s, C-3), 176.68 (s, C-4), 165.73 (s, C-5), 95.43 (d, C-6), 161.0 (s, C-7), 100.97 (d, C-8), 150.7 (s, C-9), 102.8 (s, C-10), 122.23 (s, C-1′), 129.19 (d, C-2′, 6′), 116.77 (d, C-3′, 5′), 165.7 (s, C-4′), 101.16 (d, C-1″), 73.9 (d, C-2″), 77.9 (d, C-3″), 73.22 (d, C-4″), 76.45 (d, C-5″), 182.65 (s, C-6″).[49]

2.1.2.3. Compound-IV. Yellow crystal from ethyl acetate; melting point 165−166 °C; HR-ESI + MS observed at m/z 313.10 $(M + H)^+$, calculated for $C_{18}H_{16}O_5$, 312.10. ^{1}H NMR (400 MHz, $CDCl_3$): δ ppm: 3.92 (3H, s, 6-OCH_3), 3.99 (6H, d, J = 2.7 Hz, 5 & 7-OCH_3), 6. 6 (1H, s, H-3), 6.8 (1H, s, H-8), 7.51 (3H, ddd, J = 1.84, 1.84, 4.4 Hz, H-3′, 4′, 5′), 8.22 (2H, dd, J = 5.16, 1.24Hz, H-2′, 6′). ^{13}C NMR (125 MHz, $CDCl_3$): δ ppm: 131.26 (s, C-1′), 112.96 (s, C-10), 152.63 (s, C-9), 140.42 (s, C-6), 161.11 (s, C-2), 61.53 (s, 6-OCH_3), 130.13 (s, C-4′), 128.97 (s, C-3′ & C-5′), 177.20 (s, C-4), 157.80 (s, C-7), 56.44 (s, 7-OCH_3), 125.96 (s, C-2′ & C-6′), 96.29 (s, 6-C-8), 154.57 (s, C-5), 108.41 (s, C-3), 62.18 (s, 5-OCH3).[50]

2.1.2.4. Compound-V. Yellow crystal from ethyl acetate; melting point 158−160 °C; HR-ESI + MS observed at m/z 343.11 $(M + H)^+$, calculated for $C_{19}H_{18}O_6$, 342.11. ^{1}H NMR (400 MHz, $CDCl_3$): δ ppm: 3.88 (3H, s, 6-OCH_3), 3.92 (3H, s, 4′-OCH_3), 3.98 (6H, d, J = 2.4 Hz, 5, 7-OCH_3), 6.58 (1H, s, H-3), 6.80 (1H, s, H-8), 7.01 (2H, d, J = 8.8 Hz, H-3′, 5′), 7.83 (2H, d, J = 8.8 Hz, H-2′, 6′). ^{13}C NMR (125 MHz, $CDCl_3$): δ ppm: 55.4 (s, 4-OCH_3), 56.2 (s, 7-OCH_3), 177.2 (s, C-4), 123.8 (s, C-1′), 140.3 (s, C-6), 154.5 (s, C-5), 62.2 (s, 5-OCH_3), 161.1 (s, C-4′), 107.0 (s, C-3), 114.3 (s, C-3′ & 5′),

https://doi.org/10.1021/acsomega.1c01837
ACS Omega 2021, 6, 30241−30259

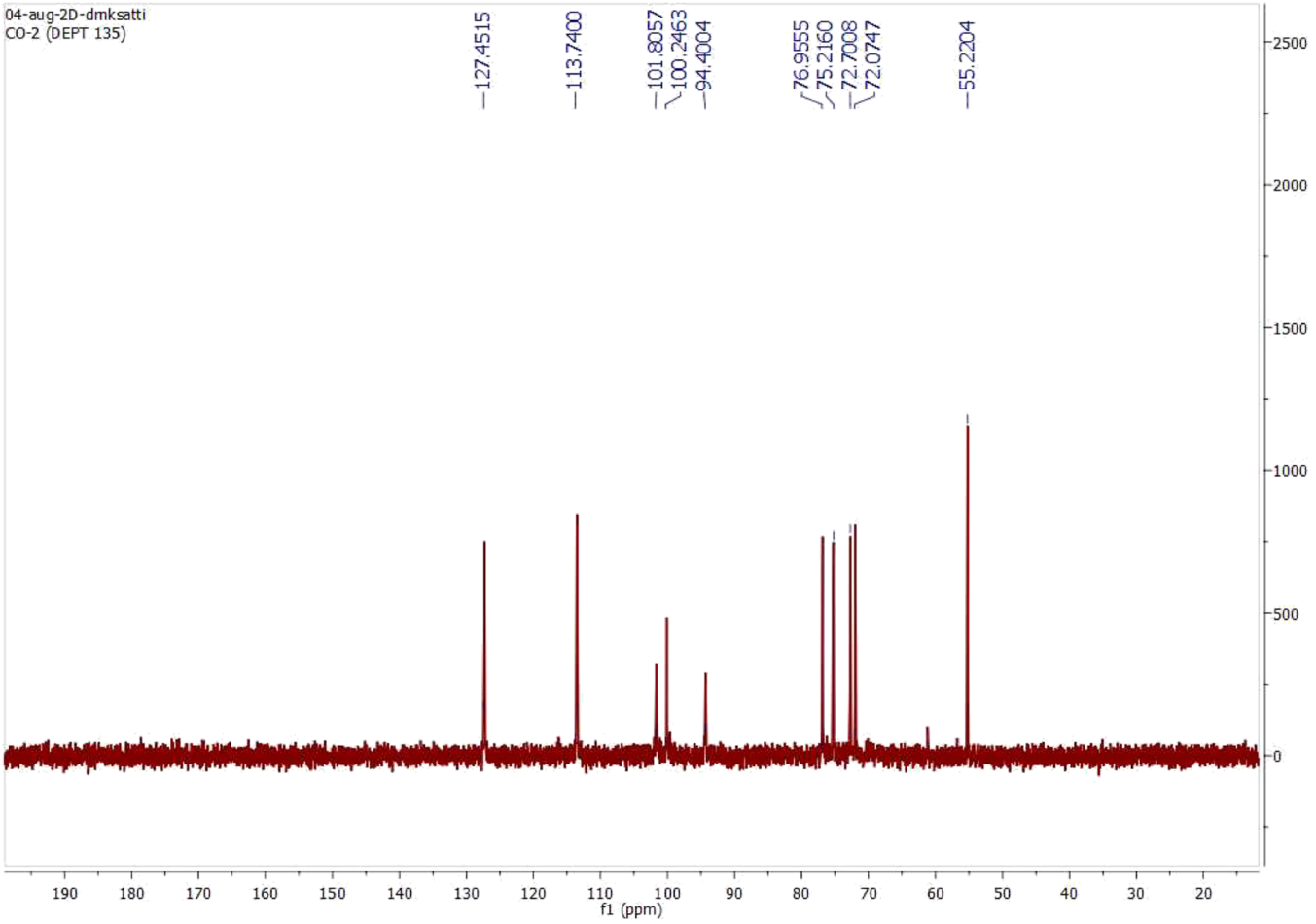

Figure 5. DEPT−NMR spectra of **III**.

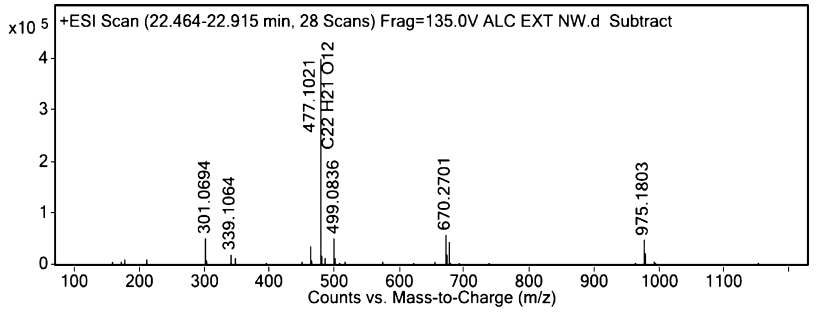

Figure 6. Mass spectra of **III**.

162.1 (s, C-2), 152.5 (s, C-8), 61.5 (s, 6-OCH_3), 112.8 (s, C-10), 127.6 (s, C-2′ & 6′), 157.6 (s, C-7).[51]

*2.1.2.5. Compound-**VI**.* Yellow crystal from ethyl acetate; melting point 230−232 °C; HR-ESI + MS observed at *m*/*z* 447.13 $(M + H)^+$, calculated for $C_{22}H_{22}O_{10}$, 446.12. ^1H NMR (400 MHz, MeOD): δ ppm: 7.48 (3H, m, H-3′, 4′ & 5′), 6.73 (1H, s, H-8), 6.79 (1H, s, H-3), 3.56 (1H, dd, *J* = 5.1, 5.0 Hz, H-6″), 3.68 (1H, dd, *J* = 2.16, 2.2 Hz, H-6″), 3.41 (1H, m, H-5″), 3.89 (3H, s, 7-OCH_3), 3.34 (3H, m, H-2″, 3″ & 4″), 4.93 (1H, d, *J* = 7.48 Hz, H-1″), 7.94 (2H, dd, *J* = 1.81, 1.32 Hz, H-2′ & 6′). ^{13}C NMR (125 MHz, MeOD): δ ppm: 136.8 (s, C-6), 130.3 (s, C-2′), 130.3 (s, C-5′), 106.0 (s, C-10), 184.5 (s, C-4), 78.6 (s, C-2″), 104.7 (s, C-3), 57.1 (s, 7-OCH_3), 75.8 (s, C-4″), 133.4 (s, C-1′), 132.0 (s, C-4′), 73.75 (s, C-5″), 126.2 (s, C-2′), 126.2 (s, C-6′), 62.3 (s, C-6″), 71.2 (s, C-3″), 153.5 (s, C-5), 151.2 (s, C-9), 105.3 (s, C-1″), 155.49 (s, C-7), 92.81 (s, C-8), 162.53 (s, C-2).[52]

*2.1.2.6. Compound-**VII**.* Yellow crystal from ethyl acetate; melting point 160−162 °C; HR-ESI + MS observed at *m*/*z* 329.1026 $(M + H)^+$, calculated for $C_{18}H_{16}O_6$, 328.09. ^1H NMR (400 MHz, $CDCl_3$): δ ppm: 7.51 (3H, t, *J* = 2.85, H-3′, 4′ & 5′), 6.51 (1H, s, H-3), 3.86 (3H, s, 8-OCH_3), 3.95 (3H, s, 7-OCH_3), 3.92 (3H, s, 7 6-OCH_3), 8.05 (dd, *J* = 3.3, 2.4 Hz). ^{13}C NMR (125 MHz, $CDCl_3$): δ ppm: 179.13 (s, C-4), 130.95 (s, C-1′), 139.55 (s, C-7), 132.39 (s, C-6), 155.94 (s, C-5), 128.63 (s, C-3′ & 5′), 152.52 (s, C-8), 158.90 (s, C-2), 56.33 (s, 7-OCH_3), 106.85 (s, C-10), 60.88 (s, 8-OCH_3), 128.38 (s, C-2′ & 6′), 60.37 (s, 6-OCH_3), 90.42 (s, C-3), 152.80 (s, C-9), 130.51 (s, C-4′).[53]

https://doi.org/10.1021/acsomega.1c01837
ACS Omega 2021, 6, 30241−30259

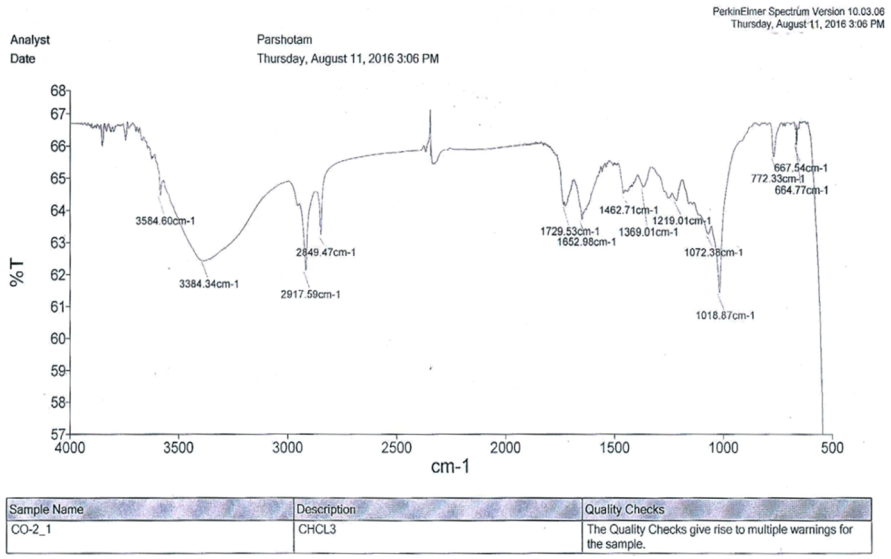

Figure 7. IR spectrum of **III**.

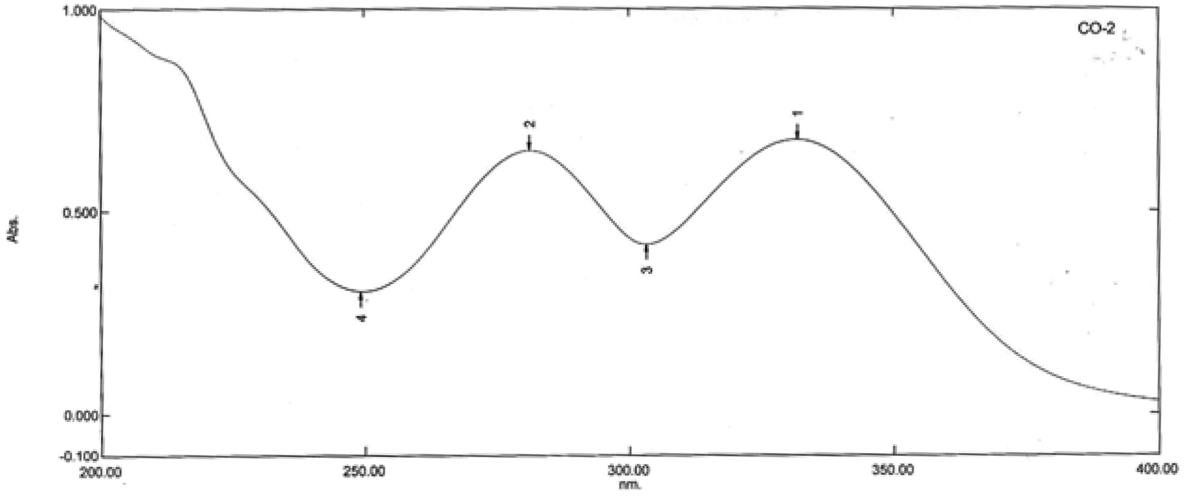

Figure 8. UV spectrum of **III**.

2.1.2.7. Compound-VIII. Yellow crystal from ethyl acetate; melting point 176−177 °C; HR-ESI + MS observed at m/z 359.1124 $(M + H)^+$, calculated for $C_{19}H_{18}O_7$, 358.10. ^{1}H NMR (400 MHz, $CDCl_3$): δ ppm: 7.02 (2H, d, J = 9.0, H-3′ & 5′), 6.50 (1H, s, H-3), 3.92 (3H, s, 4′-OCH_3), 3.86 (3H, s, 8-OCH_3), 3.95 (3H, s, 7-OCH_3), 3.90 (3H, s, 7 6-OCH_3), 8.07 (2H, d, J = 9.0 Hz, H-2′ & 6′). ^{13}C NMR (125 MHz, $CDCl_3$): δ ppm: 138.71 (s, C-7), 90.34 (s, C-3), 55.4 (s, 4-OCH_3), 114.08 (s, C-3′ & 5′), 106.60 (s, C-10), 152.34 (s, C-8), 60.13 (s, 6-OCH_3), 152.77 (s, C-9), 122.79 (s, C-1′), 60.87 (s, 8-OCH_3), 161.71 (C-2), 130.14 (s, C-2′ & 6′), 178.93 (s, C-4), 158.75 (s, C-4′), 156.0 (s, C-5), 56.31 (s, 7-OCH_3), 132.28 (s, C-6).[54]

2.1.2.8. Compound-IX. White solid from ethyl acetate; melting point 202−205 °C; HR-ESI + MS observed at m/z 447.09 $(M + H)^+$, calculated for $C_{21}H_{18}O_{11}$, 446.08. ^{1}H NMR (400 MHz, D_2O): δ ppm: 7.17 (3H, td, J = 7.2, 6.9 Hz, H-3′, 4′ & 5′), 6.17 (1H, s, H-8), 5.94 (1H, s, H-3), 3.75 (1H, d, J = 9.3 Hz, H-2″), 3.57 (1H, m, H-5″), 3.60 (1H, m, H-3″), 3.54 (1H, m, H-4″), 7.03 (2H, t, J = 6.7 Hz, H-2′ & 6′). ^{13}C NMR (125 MHz, D_2O): δ ppm: 130.81 (s, C-4′), 77.94 (s, C-2″), 76.23 (s, C-4″), 133.37 (s, C-6), 165.11 (s, C-2), 101.11 (s, C-1″), 129.96 (s, 6-C-3′ & 5′), 176.47 (s, C-6″), 150.52 (s, C-9), 146.58 (s, C-5), 183.48 (C-4), 152.09 (s, C-7), 104.40 (s, C-3), 73.12 (s, C-3″), 95.25 (s, C-8), 73.37 (s, C-5″), 106.90 (s, C-10), 130.69 (C-1′), 126.71 (s, C-2′ & 6′).[55]

(For spectra, refer to the Supporting Information of this manuscript: Figure S1−S39, Supporting Information).

2.2. Biological Evaluation. *2.2.1. Inhibitory Effect of Extracts and the Isolated Compounds on Inflammatory Cytokines and Other Inflammatory Mediators.* Proinflammatory cytokine release is an important mechanism for regulating the inflammatory responses, thus contributing to various inflammatory and autoimmune ailments. We assayed the ability of the different concentrations of the ethanolic extract (Figure 13A) and the isolated compounds (Figure S33) to decrease LPS-induced TNF-α and IL-6 production both *in vitro*[56] and *in vivo*.[57] Since the extract showed considerable downregulation of TNF-α and IL-6 both *in vivo* and *in vitro*, hence further compounds were isolated. When the whole panel of compounds was screened, it was found that compound **III** exhibited maximum inhibition, being 71.4 ± 1.4% for TNF-α and 66.3 ± 2.3% for IL-6 (Figure 13B) in the mice model. The extracts and compounds having percentage inhibition com-

https://doi.org/10.1021/acsomega.1c01837
ACS Omega 2021, 6, 30241−30259

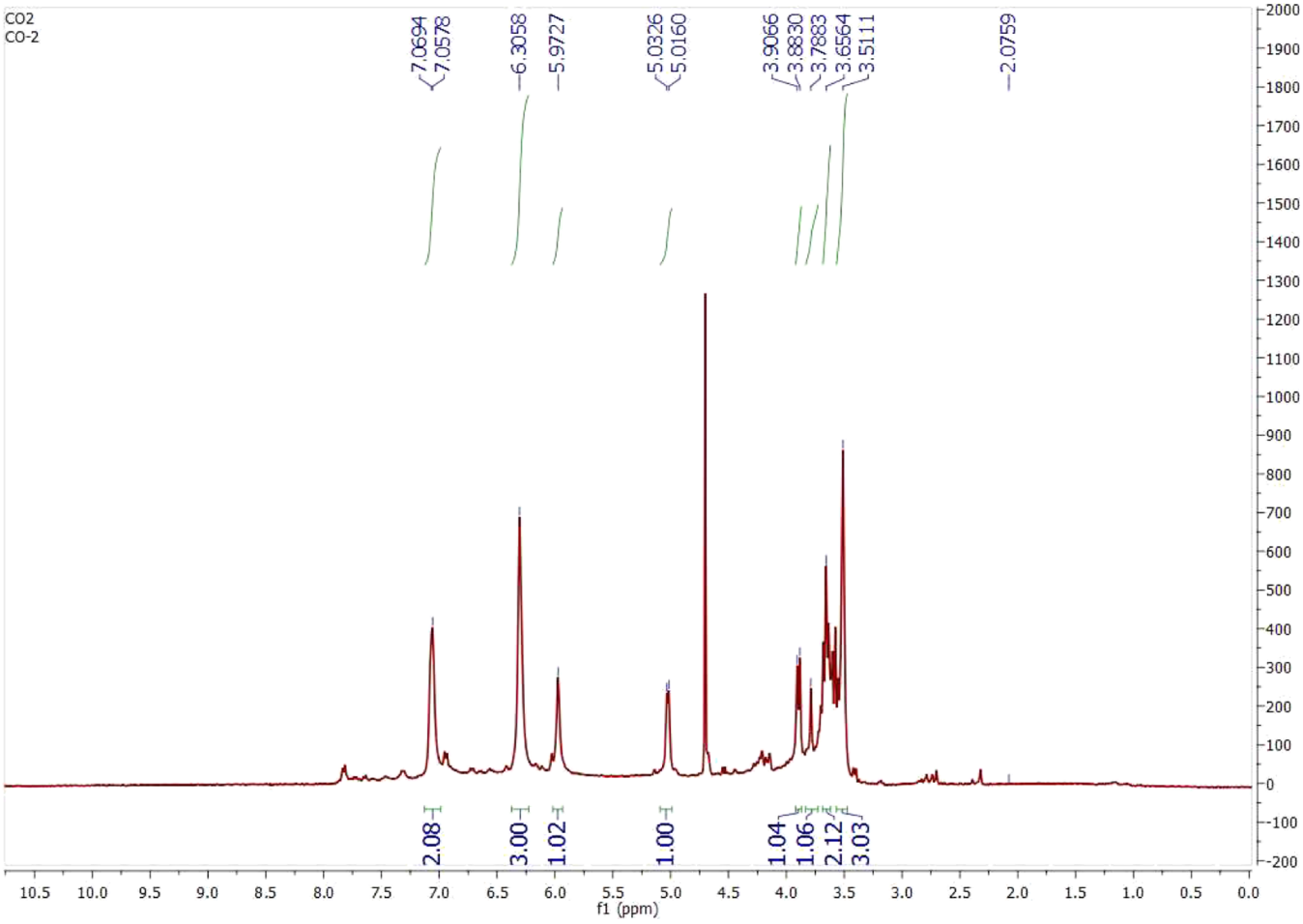

Figure 9. ^{1}H NMR spectra of **III**.

Table 2. NMR Data for III in D_2O (δ in ppm and J in Hz in Parentheses)

C-position	δ_C	δ_H	HSQC	HMBC Correlation observed in **III**	COSY	NOESY
2	163.7	Q	−C−	H-8		
3	161.6	Q	−C−	H-6′, H-3″		
4	182.3	Q	−C−	H-2″		
5	150.5	Q	−C−			
6	145.3	Q	−C−			
7	149.1	Q	−C−			
8	94.3	5.9, s, 1H	−CH−			H-2′
9	101.7	Q	−C−			
10	105.1	Q	−C−	H-8		
1′	129.9	Q	−C−	H-3′/H-5′		
2′	127.3	7.06, d, J = 4.6 Hz, 1H	−CH−		H-3′	H-3′, H-8
3′	113.5	6.3, brs, 1H	−CH−			H-2′, H-3″/H-4″
4′	121.2	7.06,d, J = 4.6 Hz, 1H	−CH−			
5′	113.5	6.3, brs, 1H	−CH−			H-1″, H-3″/H-4″
6′	127.3	7.0,d, J = 4.6 Hz, 1H	−CH−			
1″	100.1	5.02,d, J = 4.6 Hz, 1H	−CH−	H-3″, H-4″	H-3″/H-4″	H-5′, H-4″, H-2″
2″	76.8	3.8,d, J = 9.4Hz, 1H	−CH−		H-3″/H-4″	H-1″, H-4″
3″	71.9	3.6, m, 1H	−CH−	H-2″, H-5″		H-3′, H-5″
4″	72.7	3.6, m, 1H	−CH−			H-1″, H-2″
5″	75.2	3.7, m, 1H	−CH−	H-3″		H-3″
6″	175.1	Q	−C−	H-3″, H-4″		
$-OCH_3$	55.3	3.5, s, 3H	$-CH_3-$			

parable to dexamethasone were considered as active and hence could be studied further. Although all the nine molecules exhibited positive levels of inhibition of TNF-α cytokine and IL-6, compound **III** emerged as the most promising candidate

https://doi.org/10.1021/acsomega.1c01837
ACS Omega 2021, 6, 30241−30259

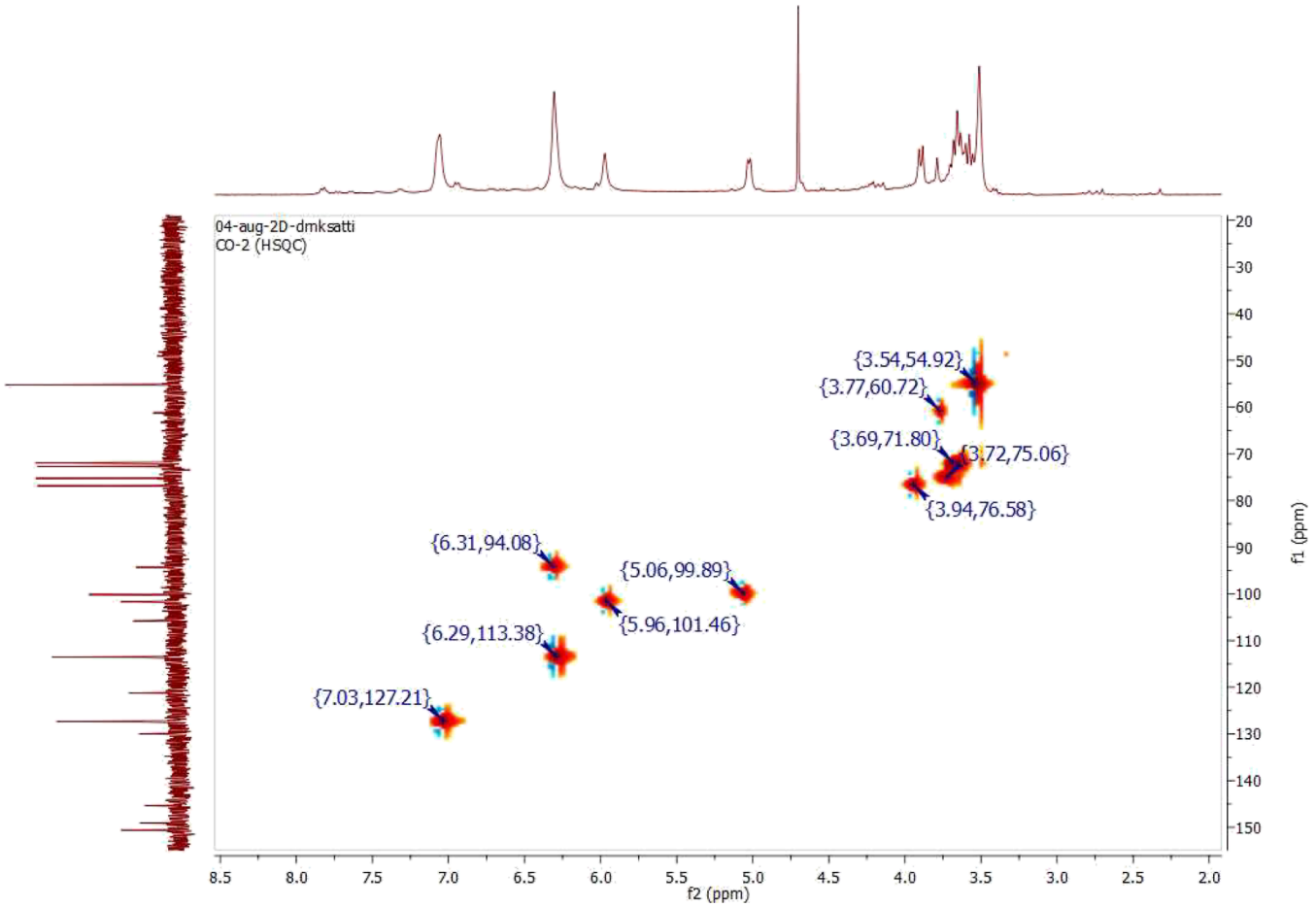

Figure 10. HSQC−NMR spectra of **III**.

for the development of an anti-inflammatory drug. Maximum inhibition of all the cytokines was observed at 10 μM. The concentration of IL-1β in compound III-treated RAW 264.7 cells was 189.1 pg/mL. Compound III inhibited gene expression of TNF-α and IL-6 in RAW 264.7 cells with reference to the housekeeping gene, glyceraldehyde 3-phosphate dehydrogenase (GAPDH) when studied through RT-PCR. To further confirm the effect of compound III, *in vivo* experiment in mice was conducted as its percentage in the serum.

In the case of IL-10, compound III treatment slightly increased its level at a concentration of 1 μM, and after that, there is a decrease in its level at 5 and 10 μM. The viability test of RAW 264.7 cells when treated with MTT assay showed no significant mortality up to a concentration of 20 μM (Figure 14). Then, we performed the *in vivo* experiments to validate the *in vitro* results. Here, the effect of compound III on the cytokine levels in LPS-stimulated Balb/c mice was studied. The *in vivo* experiments validated the *in vitro* studies and as the levels of proinflammatory cytokines TNF-α, IL-6, and IL-1β decreased with the increase in the concentration of compound III. A concentration of 5 mg/kg showed the maximum inhibition of the proinflammatory cytokines, that is, the concentration of TNF-α was 183.4 pg/mL, IL-6 was 134.2 pg/mL, IL-1β was 90.6 pg/mL, and IL-10 was 64.6 pg/mL. The effect of compound III on NO, PGE2, and LTB4 was studied in the LPS-induced RAW 264.7 cells. The results showed that these inflammatory mediators were suppressed. The maximum inhibition was at 10 μM NO: 48.6 ± 0.7 pg/mL, PGE2:779.6 ± 2.6, and LTB4:548.3 ± 5.2. The inhibition of these mediators was reasonably comparable to the standard drug dexamethasone. Compound III inhibited gene expression of iNOS and COX-2 in RAW 264.7 cells with reference to the housekeeping gene, GAPDH when studied through RT-PCR (Figures S33−S37).

2.2.2. Effects of Compound ***III*** *on LPS-Induced NF-κB p65 Expression.* RAW 264.7 cells were pretreated with compound III (1, 5, and 10 μM) for 1 h and stimulated with LPS (1 μg/mL) for 24 h. The effect on phosphorylation of IKKα/β, IKBα, and NF-kB p65 was studied with respect to dexamethasone (0.5 μM). It is clear from Figure 15 that pretreatment of compound III in the LPS-stimulated RAW264.7 cells decreased the phosphorylation of these proteins.

RAW 264.7 cells were pretreated with compound 3 (5 and 10 μM) for 1 h, LPS (1 μg/mL) was added for 24 h, and the effect on phosphorylation of NF-kB p65 was studied.

2.2.3. Effect of Compound III on Body Weight and Lymphoid Organ Weight. Compound III did not show any adverse changes in animals. Table 3 shows that the weight change in the spleen and kidney was minor in comparison to the control (normal saline treated) (group I). At 1 and 2 mg/kg, there was a slight increase in relative organ weight of the thymus but no effect at 5 mg/kg. In the case of the relative organ weight of the liver, a significant increase was observed at 2 and 5 mg/kg, while a slight increase was observed at 1 mg/kg. To confirm that the increase in liver weight is not due to

https://doi.org/10.1021/acsomega.1c01837
ACS Omega 2021, 6, 30241−30259

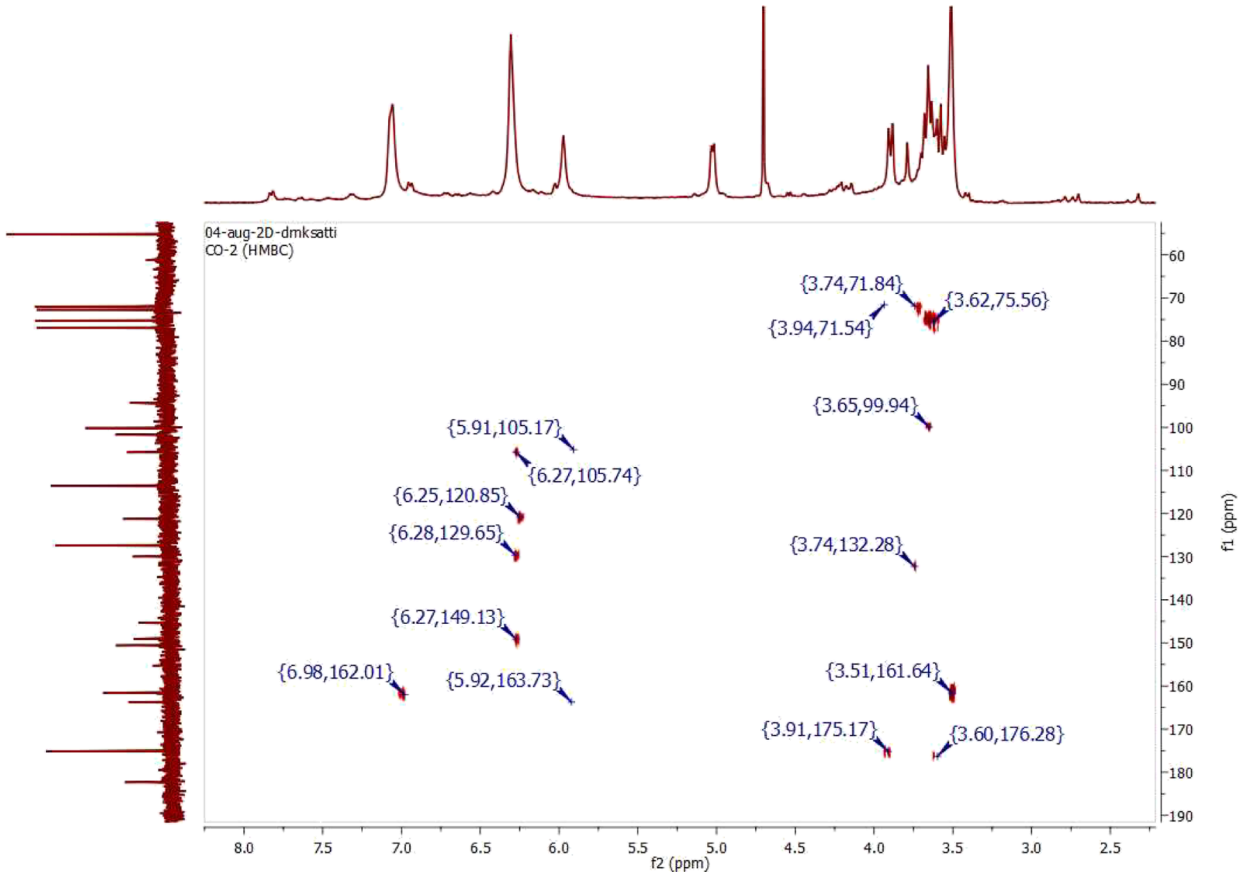

Figure 11. HMBC−NMR spectra of **III**.

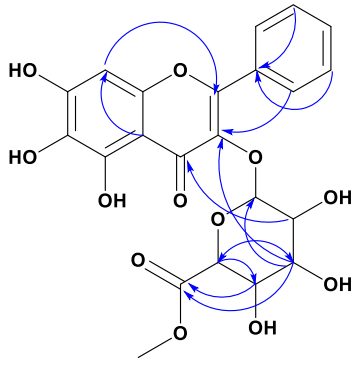

Figure 12. Major HMBC correlations in **III**, indicated by blue arrows.

any anomaly, LFTs were performed and the results do not show any aberration (Table 4).

2.2.4. Pharmacokinetic Studies of Compound III. Pharmacokinetic study was carried out following oral administration of compound III at a single dose of 10 mg/kg in BALB/c mice. The time *versus* plasma concentration profile of compound III is depicted in Figure 16. It was observed that compound III was absorbed rapidly as the time to reach maximum plasma concentration (T_{max}) after dose administration was only 15 min. The maximum plasma concentration was 11.7 ng/mL. The area under the curve for plasma concentration from zero to the last measurable plasma sample time and to infinity (AUC_{0-t} and $AUC_{0-\infty}$) was found to be 35.7 and 44.3 ng·h/mL, respectively. Plasma half-life ($T_{1/2}$) of compound III was found to be good as $T_{1/2}$ more than 2 h is sufficient for a new chemical entity to proceed for further research.

2.2.5. Histopathology. Results showed that stained liver sections of vehicle-treated animals had a central vein and a normal hepatocytic architecture. The liver of LPS-treated mice (Figure 17) had the central vein surrounded by chronic inflammation and focal hepatocytic necrosis. The inflammatory infiltrate is rich in lymphocytes and some neutrophils in the perivascular region. Compound III at a concentration of 2 mg/kg showed vascular conjection and normalization of necrosis and declined neutrophil infiltration. At a concentration of 5 mg/kg, the morphology is nearly normal.

2.2.6. Carrageenan-Induced Paw Edema and Phagocytic Index. The effect of compound III on the carrageenan-induced paw edema in the mice inflammation model was measured over a period of 10 h at doses of 1, 2, and 5 mg/kg (Figure 18). The maximum inhibition of 42.5% was observed at 5 mg/kg (Table 5). The phagocytic index (Table 6) also showed that the rate of phagocytosis increased with the increase in the concentration of compound III and is significant in comparison with the standard drug dexamethasone.

3. DISCUSSION

The goal of this work was to apply the LC−MS/MS-based dereplication method for rapid identification of unknowns in complex sample matrices with the main focus on the isolation of new chemical entities with promising biological activities and targeted isolation of unknown compounds using preparative HPLC. Structural identification of unknown compounds using NMR yielded a new compound with

https://doi.org/10.1021/acsomega.1c01837
ACS Omega 2021, 6, 30241−30259

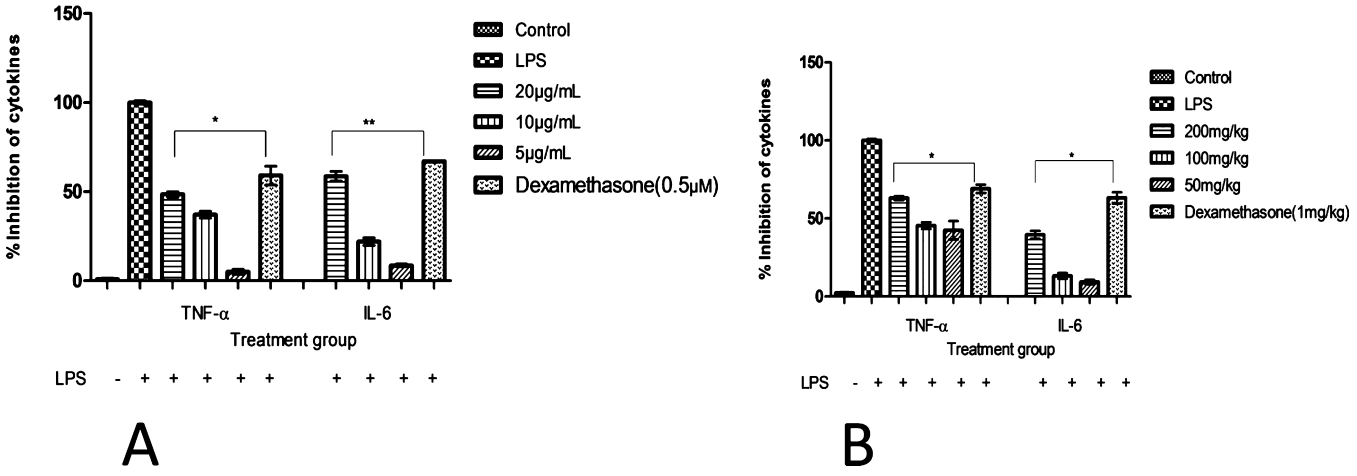

Figure 13. Cytokine assay of the ethanol extract of *C. oppositifolia*. [A] RAW 264.7 cell line was pretreated with extracts (20, 10, and 5 μg/mL) for 1 h followed by stimulation with 1 μg/mL LPS for 24 h. Production of cytokines was measured with enzyme-linked immunosorbent assay (ELISA). [B] Mice were given extracts (200, 100, and 50 mg/kg) orally for 1 h followed by LPS (0.5 mg/kg) treatment. After 3 h, blood was obtained by retro-orbital plexus (r.o.p) to collect the serum. Cytokines were measured with ELISA. Experiments were carried out in triplicates and repeated three times. Each value indicates the mean standard deviation of three independent experiments. Statistical significance was assessed by one-way ANOVA followed by Dunnett's test. *$p < 0.05$ and **$p < 0.01$ *versus* the untreated LPS-stimulated group for all the values.

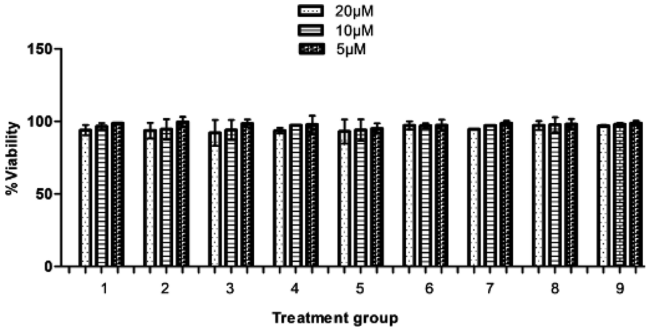

Figure 14. Viability of RAW 264.7 cells after 48 h of treatment with isolated compounds.

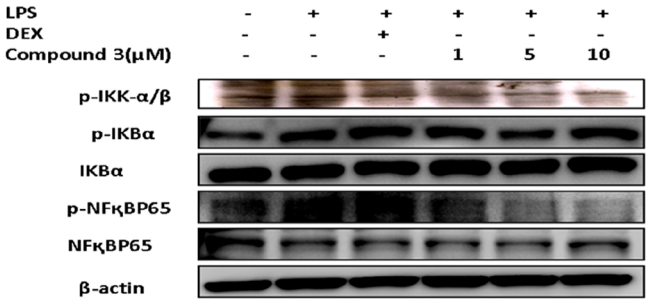

Figure 15. Inhibition of the LPS-induced phosphorylation of NF-kBp65.

Table 4. Effect of Compound III on LFTs[a]

S. no.	group	SGOT	SGPT
I	control (saline)	41.9 ± 1.2	39.2 ± 0.3
II	LPS	72.5 ± 0.9	46.6 ± 1.4
III	compound **III** (1 mg/kg)	66.3 ± 1.7	41.7 ± 1.7
IV	compound **III** (2 mg/kg)	61.2 ± 0.4	36.4 ± 0.8
V	compound III (5 mg/kg)	57.1 ± 1.4	35.2 ± 1.1

[a]Data are expressed as a mean ± standard deviation of five mice, using one way analysis of variance (ANOVA) followed by Dunnett's *t*-test.[82]

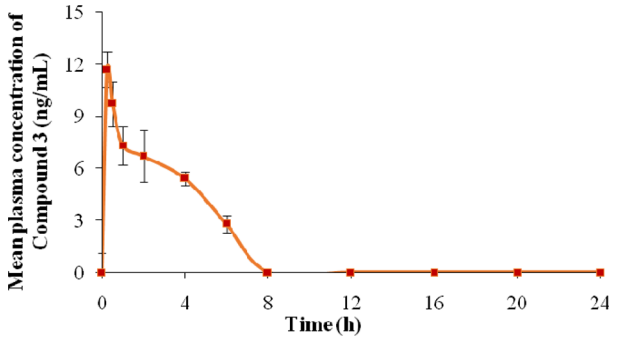

Figure 16. Time *vs* plasma concentration profile of compound III after oral administration at 10 mg/kg in BALB/c mice.

promising anti-inflammatory activity. Results of the initially conducted experiments revealed the ultimate potential of the

Table 3. Effect of Compound III on the Relative Organ Weights of Mice[a]

		relative organ weight (mean ± S.E.) in grams			
S. no.	group	spleen	thymus	liver	kidney
I	control (saline)	0.73 ± 0.4	0.17 ± 0.05	2.6 ± 0.2	1.1 ± 0.2
II	compound **III** (1 mg/kg)	0.79 ± 0.6	0.25 ± 0.03	3.4 ± 0.5	1.4 ± 0.1
III	compound **III** (2 mg/kg)	0.78 ± 0.3	0.26 ± 0.08	3.6 ± 0.7	1.37 ± 0.5
IV	compound **III** (5 mg/kg)	0.74 ± 0.2	0.19 ± 0.02	2.8 ± 0.3	1.25 ± 0.6

[a]Data are expressed as mean ± standard deviation of five mice, using Sceffe's multiple range test.

https://doi.org/10.1021/acsomega.1c01837
ACS Omega 2021, 6, 30241−30259

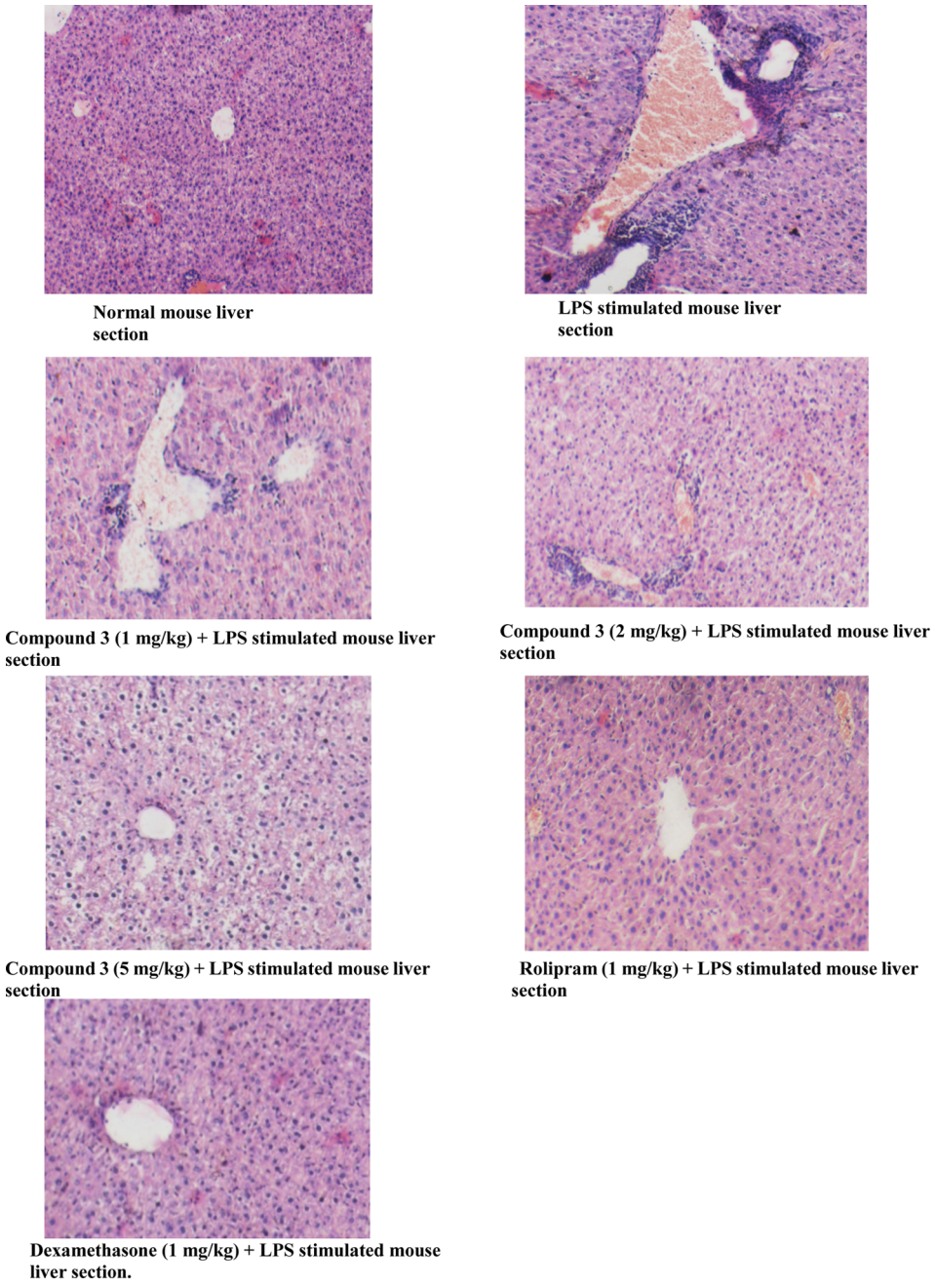

Figure 17. Photomicrographs of liver sections stained with haematoxylin and eosin (20×).

ethanol extract of *C. oppositifolia* to inhibit the proinflammatory cytokines TNF-α and IL-6. The isolated compounds significantly inhibited the proinflammatory cytokines TNF-α, IL-6, and IL-1β, whereas the anti-inflammatory cytokine IL-10 exhibited increased expression. Expression of other inflammatory mediators such as PGE2, LTB4, NO, and COX-2 was also inhibited by compound III. These results were further validated by *in silico* and *in vivo* experiments. *In vivo* results had shown considerable variation. This is due to the fact that there is only one type of cell in the *in vitro* cell culture, whereas multiple cell types exist in an organism. TNF-α, IL-6, and IL-1β are proinflammatory cytokines and are produced upon exposure to the antigen and worsen the clinical picture of disease. IL-10 is an anti-inflammatory cytokine which maintains tissue homeostasis by restricting excessive inflammatory responses.[58] The anti-inflammatory effect of IL-10 is characterized by the enhanced tissue repairing process.[59] NO and PGE_2 activate macrophages[60] and are synthesized by inducible nitric oxide synthase (iNOS) and cyclooxygenase (COX-2), respectively. Leukotrienes initiate the synthesis of particular cytokines by activating macrophages.[61] LTB4 is an early chemoattractant in the inflammatory process.[62] Our findings suggest that compound III significantly suppresses these inflammatory mediators in a dose-dependent manner. All experiments were conducted in comparison to standard drugs, dexamethasone and rolipram, and it was found that the anti-inflammatory activity of compound III is quite comparable to these standard drugs. Dexamethasone is a glucocorticoid[63−65] and binds to the glucocorticoid receptor in the cellular cytoplasm where it dimerizes and represses NF-kB tran-

https://doi.org/10.1021/acsomega.1c01837
ACS Omega 2021, 6, 30241−30259

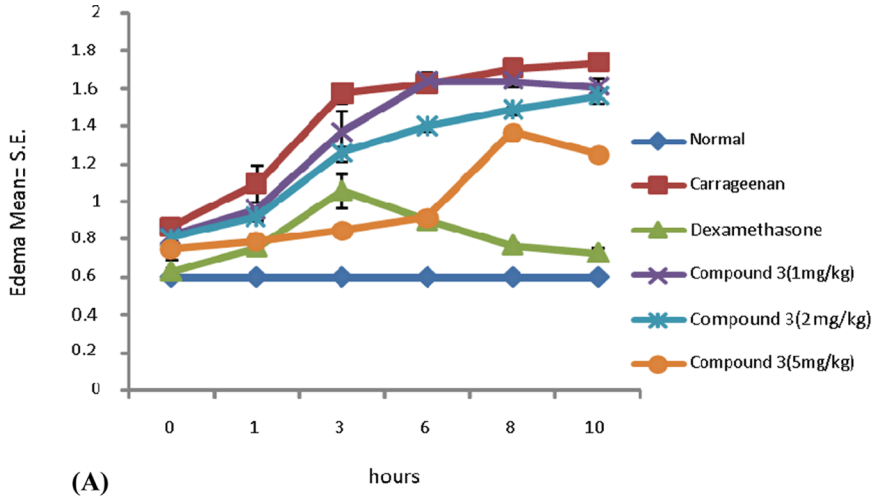

(A)

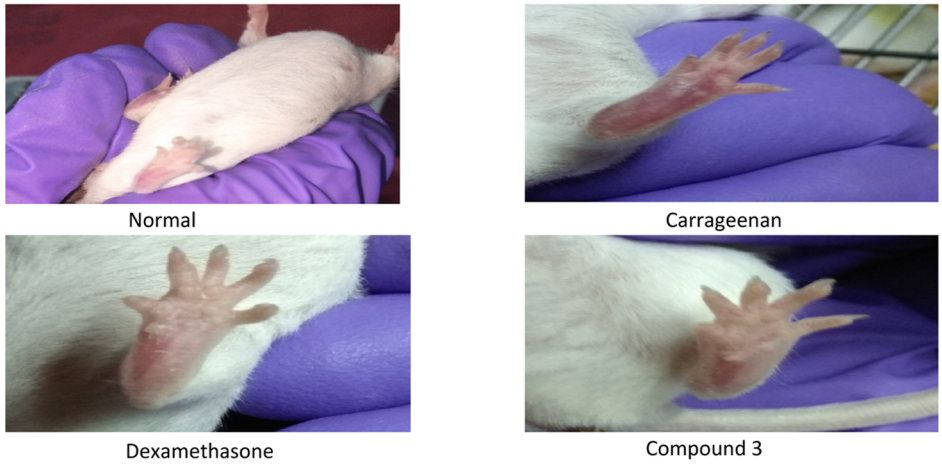

(B) Photograph courtesy of Dr. Vidushi Khajuria

Figure 18. (A): Statistical analysis. The effect of compound 3 against carrageenan-induced paw edema was measured at doses of 1, 2, and 5 mg/kg over a period of 10 h. Data are expressed as a mean standard error of five mice. (B) Anti-inflammatory activity of compound III in Balb/c mice. The effect of compound III (5 mg/kg) on the carrageenan-induced paw edema in Balb/c mice.

Table 5. Inhibition of Compound III[a]

group	percentage inhibition
compound **III** (1 mg/kg)	9.2
compound **III** (2 mg/kg)	13.8
compound **III** (5 mg/kg)	42.5
Dexamethasone (1 mg/kg)	88.5

[a]Table shows the difference between the paw volume at 0 h and 10 h and is expressed as percentage inhibition.

Table 6. Phagocytic Index[a]

group	phagocytic index
control (saline)	0.016 ± 0.003
compound III (1 mg/kg)	0.019 ± 0.001*
compound III (2 mg/kg)	0.026 ± 0.005**
compound III (5 mg/kg)	0.033 ± 0.002*
dexamethasone (1 mg/kg)	0.038 ± 0.002*

[a]Data are expressed as a mean standard deviation of five mice, using one way analysis of variance (ANOVA) followed by Dunnett's *t*-test; *$P < 0.05$ and**$P < 0.01$ versus the untreated group for all the values.

scription.[66] Rolipram is a phosphodiesterase-4 (PDE4) inhibitor. PDE4 inhibitors induce adenylate cyclase, resulting in the increase in the intracellular level of cAMP which subsequently inhibits PDE4, leading to the anti-inflammatory effect and immunomodulation.[67]

NF-κB plays a key role in the inflammatory process. In resting cells, the inhibitor of κB (IκB) protein is bound to NF-κB in the cytoplasm and is thereby inactivated. When cells receive stimuli, regulatory protein, NEMO (IKKγ), bound IKKα/β get phosphorylated. Then, the signal converges on IκB which is phosphorylated by IκB kinase, resulting in its detachment from NF-κB.

NF-κB then moves to the nucleus and thereby attaches to DNA, hence activating the transcription of a number of genes including TNF-α, iNOS, IL-6, and COX-2.[68] When LPS-treated RAW264.7 cells were treated with compound III, this signaling cascade gets blocked due to the inhibition of its phosphorylation. Thus, there was downregulation of the synthesis of both inflammatory mediators and cytokines. NF-κB is therefore considered as a target molecule for the anti-inflammatory drug development.[69] In our study, there was an increase in the level of ALT and AST enzymes which are

https://doi.org/10.1021/acsomega.1c01837
ACS Omega 2021, 6, 30241−30259

associated with liver cell destruction. However, histopathological results clearly showed that compound III restored the normal liver morphology. Macrophages phagocytose the microorganisms and dead and injured cells, thereby leading to rapid removal of parasite from blood.[70] Hence, this is a very crucial process. Phagocytic defects lead to various diseased conditions in humans.[71,72] The results clearly indicate that the phagocytic index increased significantly in comparison to control animals, thus proving the increased activity of mononuclear macrophages and also nonspecific immunity. The effect of compound III was also studied in the mice carrageenan model. This model of inflammation is used to study the effect of the test compound on various inflammatory mediators such as leukotrienes, histamine, TNF-α, nitric oxide, and so forth.[73]

Absorption across the gastrointestinal tract is considered a major determinant of pharmacological activity of any molecule. In context to this, oral pharmacokinetics of compound III was carried out at 10 mg/kg in Balb/c mice. To calculate pharmacokinetic parameters, noncompartmental analysis was used. Data depicted that it takes about 15 min (t_{max}) to reach the maximum concentration in systemic circulation, which represents its rapid absorption after oral administration. The half-life ($t_{1/2}$) of compound III was found to be 2.1 h which exhibits an acceptable pharmacokinetic profile in the mouse model.

The anti-inflammatory properties of *C. oppositifolia* may be attributed to the presence of such anti-inflammatory compounds in it. Compound **III**, being the most promising new candidate, can be further studied for the development of more effective anti-inflammatory drugs.

4. MATERIALS AND METHODS

4.1. General Experimental Procedures, Chemicals, and Biochemicals. Melting points were recorded on the digital melting point apparatus B-542 (Buchi). UV spectra were measured with a Shimadzu UV-2600 UV−vis spectrophotometer, and the IR spectra were obtained with Perkin Elmer FT-IR, Spectrum Two. ^{1}H and ^{13}C spectroscopic data were recorded on Bruker-Advance DPX FT-NMR 500 and 400 MHz instruments (125 MHz for ^{13}C NMR). LCESIMS data were acquired on an Agilent UHD-6540 LCMS/MS (HRMS) system. All the chromatographic purifications were performed on silica gel (#60−120 or #100−200 from E. Merck, Germany), SupelcoDiaion HP-20SS, USA, and Sephadex LH-20 from Sigma Aldrich. High-purity chemicals and reagents were used throughout the study. LCMS- and HPLC-grade methanol from Merck, India, HPLC-grade water from the Milli-Q water purification system, and analytical-grade acetic acid from Merck, India, were used for the analytical portions of the study. Rolipram, phosphate-buffered saline (PBS), DMEM, and carrageenan were purchased from Sigma-Aldrich. LPS *E. coli* serotype 0111:B4 and 3-(4,5-dimethylthiazole-2-yl)-2,5-diphenyltetrazolium bromide (MTT) were from Calbiochem. Fetal bovine serum was obtained from GIBCO Invitrogen Corporation. All the ELISA kits were bought from Invitrogen. The Griess reagent was purchased from Promega, and anticoagulant tubes were purchased from BD Biosciences.

4.2. Plant Material. Plant material of *C. oppositifolia* was procured from IIIM Chatha Farms, Jammu (J&K) (32.7266° N, 74.8570° E) of India, and a specimen voucher of the sample was deposited in the herbarium of the institute, that is, Janaki Ammal Herbarium (no. 22561). The powder of *C. oppositifolia* leaves (2 kg) were taken and extracted with ethanol by soxhlet extraction for 48 h on steam bath and solvent-evaporated to dryness under vacuum using a rotary evaporator at 35 °C. The yield of the ethanol extract was 12.48%. The ethanol extract was further investigated for its anti-inflammatory potential and for the isolation of active chemical constituents.

4.3. LCMS/MS-Based Isolation of Molecules. The nine molecules were isolated *via* the LCMS-based dereplication strategy whereby a highly reliable and reproducible LCMS method followed by tandem mass spectrometry, that is, MS/MS experiment, was developed for the complete separation and identification of the maximum number of compounds in the active anti-inflammatory ethanol extract of *C. oppositifolia* on the basis of parent and daughter ions generated for individual molecules. Identification of molecules was achieved by accurate mass determination and by comparing their MS/MS patterns with the ones already reported in the literature. A total of nine molecules were identified on the basis of their mass fragmentation patterns and formula generation and using the online DNP database tool. Results revealed the presence of eight known and one unknown molecule, I, II, III, IV, V, VI, VII, VIII, and IX. **III** at m/z of 477 in the positive ESI mode was expected to be a novel molecule. The LCMS method so developed was transferred to preparative HPLC, and the separated peaks were collected multiple times to obtain sufficient quantities of chemical compounds in hands in order to confirm the structural identity of the molecules by various spectroscopic techniques. Finally, the structure elucidation of the isolated compounds was carried out using different spectroscopic techniques such as nuclear magnetic resonance (NMR), infrared (IR) spectroscopy, ultraviolet (UV) spectroscopy, and mass spectrometry (MS).

4.4. Chromatographic Conditions and Apparatus. A 1200 series Agilent HPLC system equipped with a binary pump, an autosampler, an electronic degasser, a diode array detector, and a thermostatic column oven with EZchrom elite software (version 06.03 [509]) was used for the quantification and standardization of the active ethanol extract of *C. oppositifolia*. The LC separations were optimized using RP-18, Merck column (4 × 250 mm, 5 μm) where the mobile phase consisted of a mixture of methanol (B) and 2% acetic acid in water (A). HPLC was carried out in the gradient elution mode at a flow rate of 0.6 mL/min. Mobile phase B was held at 5% for the first 5 min and linearly increased to 75% in 30 min with a 5 min hold up followed by a linear decrease initially until 45 min and further for 5 min with a total run time of 50 min. The mobile phase was filtered through a 0.45 μm filter (Millipore) before use. The column temperature was maintained at 300 °C to provide sharpness to the eluting peaks. UV chromatograms were recorded at 335 nm. LC-ESI-MS analysis was performed on an Agilent LC-Q-TOF-MS (HRMS) system (Agilent Technologies, USA) equipped with Agilent HPLC 1260 series consisting of a standard autosampler (G1329B), a quaternary pump (G1311B), a thermostatted column compartment (G1316A), and diode array detector VL (G1315D) interfaced to an Agilent G6540A quadrupole time-of-flight detector with a dual ESI source. Agilent Mass Hunter qualitative analysis (B.05.00) was used for qualitative analysis. Agilent Mass Hunter workstation was used for data acquisition. Separations were achieved in a gradient mode through the Agilent RP-18 eclipse 4.6 × 100 mm (3.8 μ) column, starting with 20% methanol for 5 min with a linear increase of up to

https://doi.org/10.1021/acsomega.1c01837
ACS Omega 2021, 6, 30241−30259

75% in 25 min followed by a 5 min hold up and then a linear decrease until 20% with a total run time of 45 min. The column temperature was maintained at 30 °C. Experiment was performed both in the positive mode and in the negative mode with a gas temperature of 350 °C, drying gas flow of 12 lt/min, nebulizer 40 psi, sheath gas flow of 9 lt/min, sheath gas temp. of 350 °C, Vcap voltage of 4000 V, nozzle voltage of 1000 V, and fragmentor voltage of 135 V, and the acquisition range was set between 100 and 1200 to obtain good MS spectra. Collision-induced dissociation (CID) of 30 V was used for tandem mass spectrometry experiments.

4.5. Animals Used. About 8−10 week-old female Balb/C mice (*Mus musculus*) of 20−25 g in weight, in groups of six, were used for the *in vivo* study. Experiments were designed in a way so that a minimum number of animals were used. Experimental protocols were approved by the Institutional Animal Ethic Committee (IAEC number 861/2/16) of Indian Institute of Integrative Medicine, IIIM (CSIR), Jammu. The animals used were housed under standard laboratory conditions at a temperature of 23 ± 1 °C, relative humidity of 55 ± 10%, and light/dark cycles of 12/12 h, fed with the standard pellet diet (Lipton India Ltd), and received water ad libitum. None of the animals was sacrificed throughout the study; however, as per the institute's norms, they were subjected to euthanasia after the experimentation using diethyl ether and were disposed off by means of incineration. Standard and testing extracts and compounds used for the *in vivo* study were dissolved in 100% dimethyl sulfoxide (DMSO), but the working concentration of DMSO was made in such a way that below 1% was injected into the animals.

4.6. Cell Culture. Murine macrophages cells (RAW 264.7) were obtained from NCCS, Pune, India, cultured in DMEM medium containing 10% fetal bovine serum (FBS) and penicillin−streptomycin (GIBCO) at 37 °C in a humidified 5% CO_2 atmosphere. The actual concentration of DMSO in the treated plate was 0.1%.

4.7. Biological Assays. *4.7.1. Effect of the Extract and Compound III on Cytokine Production (TNF-α, IL-6, IL-1β, and IL-10) and Proinflammatory Mediators (NO, PGE2, and LTB4) in RAW 264.7 Cells and Balb/C Mice.* The inhibitory effect of the extract and the compounds was determined by ELISA. RAW 264.7 cells were seeded into a 96-well plate at a density of 2×10^5 cells/well and incubated overnight. The cells were then treated with the corresponding extract (20, 10, and 5 μg/mL) and compounds (10, 5, and 1 μM) with a volume of 90 μL for 1 h followed by the addition of 1 μg/mL (10 μL) LPS for 24 h to induce inflammation. Culture supernatants were assayed as per the protocol of the ELISA kit to measure the amount of cytokines produced in each sample. The experiment was carried out in triplicate.

Overnight-fasted mice were drugged orally with the test extract (200, 100, and 50 mg/kg) and compounds (5, 2, and 1 mg/kg) for 1 h. LPS (0.5 mg/kg) was administered *via* intraperitoneal (i.p.) injection. Blood was collected after 3 h from the retro-orbital plexus (r.o.p). Serum was collected and stored at −80 °C until used for ELISA[74] to study the inhibition of cytokines using Invitrogen (Mouse) kits. For the measurement of NO, PGE2, and LTB4, the protocol followed by Khajuria *et al.*, 2018[75] was used.

4.7.2. MTT Assay for Measurement of Cell Viability. RAW 264.7 cells (16,000 cells/well) were treated with different concentrations (5, 10, and 20 μM) of compounds (Figure 14) for 48 h in flat-bottomed microtiter plates. MTT solution (20 μL, 2.5 mg/mL) prepared in PBS, pH 7.4 was added 4 h prior to culture termination. 100% DMSO (100 μL) was added in each well to solubilize the formazan. Absorbance was measured at a wavelength of 570 nm using a Synergy Mx plate reader. The LPS-treated group was used as the control in calculating percentage cell viability.

$$\text{cell viability (\%)} = (\text{OD}_{\text{control}} - \text{OD}_{\text{sample}})/\text{OD}_{\text{control}}$$

4.7.3. Pharmacokinetic Study of Compound III. Single-dose oral pharmacokinetic study of compound III was carried out using healthy adult BALB/c. Twenty animals were kept under standard laboratory conditions with water *ad libitum* for a period of 1 week before experimentation. Animals were fasted overnight and divided into four groups containing five animals per group on the day of experimentation. The dose was prepared in 5% DMSO, 30% solutol HS-15, 20% polyethylene glycol (PEG) 400, and 45% water (v/v) and administered through the oral route at 10 mg/kg with a dose volume of 10 mL/kg. Blood samples were collected from retero-orbital plexus of at 0 (predose), 0.25, 0.5, 1, 2, 4, 6, and 8 h in microcentrifuge tubes containing 5% (w/v) disodium EDTA. Two blood samples were collected from each group to execute pharmacokinetic study using the sparse sampling technique. Each blood sample was centrifuged at 10,643*g* for 10 min to obtain each of 50 μL plasma which was further processed with methanol (200 μL) for plasma protein precipitation. Then, the sample was mixed thoroughly by vortexing for 2 min followed by centrifugation at 14000 rpm for 10 min at 4 °C. The organic layer was separated and transferred to the HPLC vial for analysis. Compound III was dissolved in DMSO and diluted further with methanol to obtain a calibration curve (0.48−500 ng/mL) by spiking an appropriate amount into the blank plasma. Quantitation of compound III was carried out using LC−MS/MS (Make: Shimadzu; model: 8030). Separation was achieved in a Chromolith high-resolution RP-18e column (50 × 4.6 mm) (Merck-Millipore) using mobile-phase composition of water with 0.1% formic acid, v/v (solvent A) and acetonitrile (solvent B) at a flow rate of 0.3 mL/min. Gradient elution was programmed as follows: 0.01−2 min, 10% B; 2−4 min, 10−60% B; 4−6 min, 60% B; 6−8 min, 60−10% B; and 8−10 min, 10%. A tandem mass spectrophotometer with an electrospray ionization (ESI) source was operated in the positive mode, and quantitation of compound III was performed in the multiple reaction monitoring (MRM) mode with parent ion/product ion transition pairs of 477.1 > 301.2. Plasma concentrations of compound III at the respective time points were obtained, and calculation was carried out for various pharmacokinetic parameters by noncompartmental analysis using PK solution software (Summit Research Services, Colorado, USA).

4.7.4. Western Blotting. RAW 264.7 cells (2×10^5cells/well) were pretreated with compound III (5 and 10 μM) for 1 h and stimulated with LPS (1 μg/mL) for 24 h. Cells were then harvested; then, the cell pellet was dissolved in radioimmunoassay precipitation buffer (Sigma; R-0278) over ice for 40 min. The lysate was then centrifuged at 14,000*g* for 15 min at 4 °C, and the supernatant was collected. Protein estimation was carried out by Bradford's method with the bovine serum albumin (BSA) standard. Western blotting was performed according to the reported protocol.[76] Specific proteins were detected by Immobilon Western (Chemiluminescent HRP substrate, Millipore)-mediated chemiluminescence by Chem-iDoc XRS+ (Bio Rad). Densitometric analysis of specific bands

https://doi.org/10.1021/acsomega.1c01837
ACS Omega 2021, 6, 30241−30259

was carried out using Image Lab Software version 3 (Bio Rad). The effect on phosphorylation of IKK-α/β, IKBα, and NF-kB p65 was studied in a dose-dependent manner with respect to dexamethasone (0.5 μM).

4.7.5. Total RNA Extraction. Total cellular RNA was isolated from RAW 264.7 cells using a Quiagen RNeasy Mini Kit. cDNAs were synthesized from 1 μg of RNA of each sample using a Superscript vilo cDNA synthesis kit following the manufacturer's protocol. The PCR cycle involved incubation at 25 °C for 10 min following 42 °C for 1 h and termination at 85 °C for 5 min. The Q-RT-PCR was carried out in a 20 μL final volume containing 1 μL of the synthesized cDNA sample, 2.5 μM primer pairs, and 10 μL of SYBR green PCR master mix in Roche Light Cycler real-time PCR systems. The following protocol was followed, 50 °C for 2 min followed by 40 cycles at 95 °C for 10 min and then 95 °C for 15 s and 60 °C for 1 min using the following primers. Relative expression levels of the target genes were calculated based on $2^{-\Delta\Delta Ct}$ according to the manufacture's specifications using the glyceraldehyde 3-phosphate dehydrogenase (GAPDH) gene as a reference housekeeping gene.[77,78] The primer sequence is TNF-α-sense (5′-CTCCAGGCGGTGCC-TATGT-3′), TNF-α-antisense (5′-GAA-GAGCGTGGTGGCCC-3′), IL-6-sense (5′-CCA-GAAACCGCTATGAAGTTCC-3′), IL-6-antisense (5′-TCACCAGCATCAGTCCCAAG-3′), iNOS-sense (5′-TCACTGGGACAGCACAGAAT-3′), iNOS-antisense (5′-TGTGTCTGCAGATGTGCTGA-3′), COX-2-sense (5′-GGGAAGCCTTCTCCAACC-3′), COX-2-antisense (5′-GAACCCAGGTCCTCGCTT-3′), GAPDH-sense (5′-TGTGTCCGTCGTGGATCTGA-3′), and GAPDH-antisense (5′-TGCCTGCTTCACCACCTTCT-3′).

4.7.6. Body Weight and Lymphoid Organ Weight. Animals were divided into four experimental groups (I–IV) each having five animals (Table 3): group I (control), normal saline; group II, compound III (1 mg/kg body weight); group III, compound III (2 mg/kg); and group IV, compound III (5 mg/kg). Animals were sacrificed 24 h after the last dose. Body weight gain (percentage) and relative organ weight (organ weight/100 g of body weight) of the spleen, thymus, liver, and kidney for each animal were determined.[79]

4.7.7. Liver Function Test. Animals were divided into five groups comprising five animals each. Group I (control) received normal saline; group II received LPS (0.5 mg/kg), and the rest of the groups received the respective doses of compound III for 5 days (Table 4). Serum glutamate oxalate transaminase (SGOT) and serum glutamate pyruvate transaminase (SGPT) were measured using the kits (Erba Diagnostics, India).

4.7.8. Histopathology. After the completion of experiment, animals were sacrificed by decapitation. Then, the liver was removed from the animals, sliced, and subsequently washed in saline. A small part of liver tissue was preserved in 10% formalin. The tissues were embedded in paraffin wax and sectioned to 4 to 5 μm thickness using a microtome. The sections were subjected to histopathological studies after haematoxylin and eosin staining and then photographed.[80]

4.7.9. Efficacy of Compound III against Carrageenan-Induced Paw Edema. Six groups of mice (n = 5) were fasted overnight and treated orally with compound III (1, 2, and 5 mg/kg). 1% carrageenan solution (100 μL) was prepared in PBS and injected at the subplantar region of the left hind paw of all animals. Then, the volume of the injected paw was measured using a plethysmometer at 1, 3, 6, 8, and 10 h. The percentage inhibition of paw edema was calculated using the following formula

$$\text{oedema (\%) inhibition} = (V_c - V_t/V_c) \times 100$$

V_c—volume of paw edema in the control group. V_t—volume of paw edema in the treated group.

4.7.10. Macrophage Phagocytosis by the Carbon Clearance Method. On day 6, all the groups were given 0.1 mL of carbon ink suspension through the tail vein. Blood was collected from the retro-orbital plexus at 0 and 30 min immediately after the injection of carbon suspension. Blood was lysed with 2 mL of 0.1% sodium carbonate, and the absorbance was measured at 675 nm.[81] The rate of carbon clearance, termed as the phagocytic index, was calculated using the equation.[82]

$$\text{phagocytic index} = (\ln \text{OD}_1 - \ln \text{OD}_2)/t_2 - t_1$$

OD1: optical density at a time (t_1) 0 min after blood collection from mice tail vein. OD2: optical density at a time (t_2) 30 min after blood collection from mice tail vein.

4.7.11. Statistical Analysis. Data were expressed as mean ±S.E.M., using one-way analysis of variance (ANOVA) followed by Dunnett's t-test. All the statistical analysis has been carried out using Graphpad Prism software which calculates the P-value also.

■ ASSOCIATED CONTENT

Supporting Information

The Supporting Information is available free of charge at https://pubs.acs.org/doi/10.1021/acsomega.1c01837.

NMR, HRMS, and HPLC data of compounds (I to IX), *in vitro* and *in vivo* assays of the other eight isolated compounds, effects of compound **III** on the mRNA levels of the inflammatory factors TNF-α and IL-6 and COX-2 and iNOS, inhibition of the LPS-induced IL-1β production in RAW 264.7 cells and Balb/c mice; IL-10 production in RAW 264.7 cells and Balb/c mice, and inhibition of the LPS-induced NO, PGE2, and LTB4 production by compound **III** in RAW 264.7 (PDF)

■ AUTHOR INFORMATION

Corresponding Authors

Mahendra Kumar Verma − *Natural Product Chemistry Division, Analytical Chemistry Division, CSIR-Indian Institute of Integrative Medicine, Jammu 180001, India;* orcid.org/0000-0002-9961-8382; Phone: +91 191-2585006-12 Ext.472/460; Email: mkvermadr@yahoo.com, mkverma@iiim.res.in, mkverma@iiim.ac.in

Naresh Kumar Satti − *Natural Product Chemistry Division, Analytical Chemistry Division, CSIR-Indian Institute of Integrative Medicine, Jammu 180001, India*; Phone: +91 191-2585006-12 Ext.218; Email: nksatti@gmail.com

Zabeer Ahmed − *Inflammation Pharmacology Division, CSIR-Indian Institute of Integrative, Jammu 180001, India; AcSIR: Academy of Scientific and Innovative Research, Jammu 180006, India*; Phone: +91 191-2585006-12 Ext.205; Email: zahmed@iiim.ac.in

Authors

Neha Sharma − *Natural Product Chemistry Division, Analytical Chemistry Division, CSIR-Indian Institute of*

https://doi.org/10.1021/acsomega.1c01837
ACS Omega 2021, 6, 30241−30259

Integrative Medicine, Jammu 180001, India; Present Address: Advanced Technology Platform Centre, Regional Centre for Biotechnology, Faridabad, Haryana, India

Vidushi Khajuria − *Inflammation Pharmacology Division, CSIR-Indian Institute of Integrative, Jammu 180001, India; AcSIR: Academy of Scientific and Innovative Research, Jammu 180006, India*

Shilpa Gupta − *Inflammation Pharmacology Division, CSIR-Indian Institute of Integrative, Jammu 180001, India; AcSIR: Academy of Scientific and Innovative Research, Jammu 180006, India;* Present Address: Research Associate, Harm Reduction and Innovation Center, Lower Parel, Mumbai 400013, India.

Chetan Kumar − *Natural Product Chemistry Division, Analytical Chemistry Division, CSIR-Indian Institute of Integrative Medicine, Jammu 180001, India*

Anjana Sharma − *AcSIR: Academy of Scientific and Innovative Research, Jammu 180006, India; PK-PD and Toxicology Division, CSIR-Indian Institute of Integrative Medicine, Jammu 180006, India;* Present Address: Pharmacovigilance Associate, Department Of Pharmacology, Dr. Radhakrishnan Government Medical College, Hamirpur, Himachal Pradesh, India.

Nazir Ahmad Lone − *AcSIR: Academy of Scientific and Innovative Research, Jammu 180006, India; PK-PD and Toxicology Division, CSIR-Indian Institute of Integrative Medicine, Jammu 180006, India*

Satya Paul − *Department of Chemistry, University of Jammu, Jammu 180006, India;* orcid.org/0000-0002-9859-3371

Siya Ram Meena − *Genetic Resource & Agrotech. Division, CSIR-Indian Institute of Integrative Medicine, Jammu 180001, India*

Complete contact information is available at: https://pubs.acs.org/10.1021/acsomega.1c01837

Author Contributions

[¶]N.S. and V.K. contributed equally.

Funding

This work was supported by Council of Scientific and Industrial Research (CSIR), New Delhi, India.

Notes

The authors declare no competing financial interest.

■ ACKNOWLEDGMENTS

Two authors N.S. and V.K. are highly thankful to the Department of Science and Technology, New Delhi, for the award of INSPIRE fellowship. We are also thankful to CSIR for financial support under project BSC-0110. We also acknowledge the institutional publication number CSIR−IIIM/1809/2018.

■ REFERENCES

(1) Eldridge, G. R.; Vervoort, H. C.; Lee, C. M.; Cremin, P. A.; Williams, C. T.; Hart, S. M.; Goering, M. G.; O'Neil-Johnson, M.; Zeng, L. High-throughput method for the production and analysis of large natural product libraries for drug discovery. *Anal. Chem.* **2002**, *74*, 3963−3971.

(2) Butler, M. S. Natural products to drugs: natural product-derived compounds in clinical trials. *Nat. Prod. Rep.* **2008**, *25*, 475−516.

(3) Morrison, K. C.; Hergenrother, P. J. Natural products as starting points for the synthesis of complex and diverse compounds. *Nat. Prod. Rep.* **2014**, *31*, 6−14.

(4) Berlinck, R. G. S. Review of Natural Products Isolation. *J. Nat. Prod.* **2017**, *80*, 2590.

(5) Joyner, P. M.; Cichewicz, R. H. Bringing natural products into the fold−exploring the therapeutic lead potential of secondary metabolites for the treatment of protein-misfolding-related neurodegenerative diseases. *Nat. Prod. Rep.* **2011**, *28*, 26−47.

(6) Baker, D. D.; Chu, M.; Oza, U.; Rajgarhia, V. The value of natural products to future pharmaceutical discovery. *Nat. Prod. Rep.* **2007**, *24*, 1225−1244.

(7) Butler, M. S. The role of natural product chemistry in drug discovery. *J. Nat. Prod.* **2004**, *67*, 2141−2153.

(8) Cieśla, Ł.; Moaddel, R. Comparison of analytical techniques for the identification of bioactive compounds from natural products. *Nat. Prod. Rep.* **2016**, *33*, 1131−1145.

(9) Silva Elipe, M. V. Advantages and disadvantages of nuclear magnetic resonance spectroscopy as hyphenated technique. *Anal. Chim. Acta* **2003**, *497*, 1−25.

(10) Murakami, T.; Kawasaki, T.; Takemura, A.; Fukutsu, N.; Kusu, F. Identification of degradation products in loxoprofen sodium adhesive tapes by liquid chromatography-mass spectrometry and dynamic pressurized liquid extraction-solid-phase extraction coupled to liquid chromatography-nuclear magnetic resonance spectroscopy. *J. Chromatogr. A* **2008**, *1208*, 164−174.

(11) Norwood, D. L.; Mullis, J. O.; Davis, M.; Pennino, S.; Egert, T.; Gonnella, N. C. Automated Solid Phase Extraction (SPE) LC/NMR Applied to the Structural Analysis of Extractable Compounds from a Pharmaceutical Packaging Material of Construction. *PDA J. Pharm. Sci. Technol.* **2013**, *67*, 267−287.

(12) Weber, B.; Hartmann, B.; Stöckigt, D.; Schreiber, K.; Roloff, M.; Bertram, H.-J.; Schmidt, C. O. Liquid chromatography/mass spectrometry and liquid chromatography/nuclear magnetic resonance as complementary analytical techniques for unambiguous identification of polymethoxylated flavones in residues from molecular distillation of orange peel oils (Citrus sinensis). *J. Agric. Food Chem.* **2006**, *54*, 274−278.

(13) Madhavan, V.; Yadav, D. K.; Gurudeva, M.; Yoganarasimhan, S. Pharmacognostical studies on the leaves of *Colebrookea oppositifolia* Smith. *Asian J. Tradit. Med.* **2011**, *6*, 134−144.

(14) Venkateshappa, S. M.; Sreenath, K. P. Potential medicinal plants of lamiaceae. *AIJRFANS* **2013**, *3*, 82−87.

(15) Kumar, M.; Bussmann, R. W.; Mukesh, J. Ethnomedicinal uses of plants close to rural habitation in Garhwal Himalaya. India. *J. Med. Plants Res.* **2011**, *5*, 2252−2260.

(16) Mittal, A.; Satish, S.; Anima, P. Herbal boon for wounds. *Int. J. Pharm. Sci.* **2013**, *5*, 1−12.

(17) Ishtiaq, S.; Meo, M. B.; Afridi, M. S. K.; Akbar, S.; Rasool, S. Pharmacognostic studies of aerial parts of Colebrookea oppositifolia Sm. *Ann. Phytomed.* **2016**, *5*, 161−167.

(18) Gupta, R. S.; Yadav, R. K.; Dixit, V. P.; Dobhal, M. P. Antifertility studies of *Colebrookea oppositifolia* leaf extract in male rats with special reference to testicular cell population dynamics. *Fitoterapia* **2001**, *72*, 236−245.

(19) Joshi, K.; Joshi, R.; Joshi, A. R. Indigenous knowledge and uses of medicinal plants in Macchegaun, Nepal. *Indian J. Tradit. Knowl.* **2011**, *10*, 281−286.

(20) Poudel, S. K. Ethnobotanical Study of the Tharus Living in Central Part of Dang (Mid-Western Nepal). M. Sc. Dissertation, Tribhuvan University, Kirtipur, Nepal, 2000.

(21) Malla, B.; Chhetri, R. B. Indigenous knowledge on ethnobotanical plants of Kavrepalanchowk district. *Kathmandu University Journal of Science, Engineering and Technology* **2009**, *5*, 96−109.

(22) Singh, S. P.; Singh, S. K.; Tripathi, S. C. Antifungal activity of essential oils of some Labiatae plants against dermatophytes. *Indian Perfum.* **1983**, *27*, 171−173.

(23) Smolen, J. S.; Steiner, G. Therapeutic strategies for rheumatoid arthritis. *Nat. Rev. Drug Discovery* **2003**, *2*, 473−488.

(24) Newton, R. C.; Decicco, C. P. Therapeutic Potential and Strategies for Inhibiting Tumor Necrosis Factor-α. *J. Med. Chem.* **1999**, *42*, 2295−2314.

(25) Hotamisligil, G. S.; Arner, P.; Caro, J. F.; Atkinson, R. L.; Spiegelman, B. M. Increased adipose tissue expression of tumor necrosis factor-alpha in human obesity and insulin resistance. *J. Clin. Invest.* **1995**, *95*, 2409−2415.
(26) Selmaj, K.; Raine, C. S.; Cannella, B.; Brosnan, C. F. Identification of lymphotoxin and tumor necrosis factor in multiple sclerosis lesions. *J. Clin. Invest.* **1991**, *87*, 949−954.
(27) Lovering, F.; Zhang, Y. Therapeutic potential of TACE inhibitors in stroke. *CNS Neurol. Disord.: Drug Targets* **2005**, *4*, 161−168.
(28) Rösler, N.; Wichart, I.; Jellinger, K. A. Intra vitam lumbar and post mortem ventricular cerebrospinal fluid immunoreactive interleukin-6 in Alzheimer's disease patients. *Acta Neurol. Scand.* **2001**, *103*, 126−130.
(29) Such, J.; Hillebrand, D. J.; Guarner, C.; Berk, L.; Zapater, P.; Westengard, J.; Peralta, C.; Soriano, G.; Pappas, J.; Runyon, B. A. Tumor necrosis factor-alpha, interleukin-6, and nitric oxide in sterile ascitic fluid and serum from patients with cirrhosis who subsequently develop ascitic fluid infection. *Dig. Dis. Sci.* **2001**, *46*, 2360−2366.
(30) Ruiz-Alcaraz, A. J.; Martínez-Esparza, M.; Caño, R.; Hernández-Caselles, T.; Recarti, C.; Llanos, L.; Zapater, P.; Tapia, A.; Martín-Orozco, E.; Pérez-Mateo, M.; Such, J.; García-Peñarrubia, P.; Francés, R. Peritoneal macrophage priming in cirrhosis is related to ERK phosphorylation and IL-6 secretion. *Eur. J. Clin. Invest.* **2011**, *41*, 8−15.
(31) Jahromi, M. M.; Millward, B. A.; Demaine, A. G. A polymorphism in the promoter region of the gene for interleukin-6 is associated with susceptibility to type 1 diabetes mellitus. *J. Interferon Cytokine Res.* **2000**, *20*, 885−888.
(32) Lenon, G. B.; Xue, C. C. L.; Story, D. F.; Thien, F. C.; McPhee, S.; Li, C. G. Inhibition of release of inflammatory mediators in primary and cultured cells by a Chinese herbal medicine formula for allergic rhinitis. *Chin. Med.* **2007**, *2*, 2.
(33) Henderson, W. R. The role of leukotrienes in inflammation. *Ann. Intern. Med.* **1994**, *121*, 684−697.
(34) Lewis, R. A.; Austen, K. F.; Soberman, R. J. Leukotrienes and other products of the 5-lipoxygenase pathway. biochemistry and relation to pathobiology in human diseases. *N. Engl. J. Med.* **1990**, *323*, 645−655.
(35) Funk, C. D. Prostaglandins and leukotrienes: advances in eicosanoid biology. *Science* **2001**, *294*, 1871−1875.
(36) Molloy, R. G.; Mannick, J. A.; Rodrick, M. L. Cytokines, sepsis and immunomodulation. *Br. J. Surg.* **1993**, *80*, 289−297.
(37) Hinz, B.; Brune, K. Cyclooxygenase-2-10 years later. *J. Pharmacol. Exp. Ther.* **2002**, *300*, 367−375.
(38) Guslandi, M. Nitric oxide and inflammatory bowel diseases. *Eur. J. Clin. Invest.* **1998**, *28*, 904−907.
(39) MacMicking, J.; Xie, Q.-w.; Nathan, C. Nitric oxide and macrophage function. *Annu. Rev. Immunol.* **1997**, *15*, 323−350.
(40) Prescott, S. M.; Fitzpatrick, F. A. Cyclooxygenase-2 and carcinogenesis. *Biochim. Biophys. Acta* **2000**, *1470*, M69−M78.
(41) Akira, S.; Takeda, K.; Kaisho, T. Toll-like receptors: critical proteins linking innate and acquired immunity. *Nat. Immunol.* **2001**, *2*, 675.
(42) De Groote, M. A.; Gruppo, V.; Woolhiser, L. K.; Orme, I. M.; Gilliland, J. C.; Lenaerts, A. J. Importance of confirming data on the in-vivo efficacy of novel antibacterial drug regimens against various strains of Mycobacterium tuberculosis. *Antimicrob. Agents Chemother.* **2012**, *56*, 731−738.
(43) Yang, F.; Li, X.-C.; Wang, H.-Q.; Yang, C.-R. Flavonoid Glycosides from *Colebrookea oppositifolia*. *Phytochemistry* **1996**, *42*, 867−869.
(44) Patwardhan, S. A.; Gupta, A. S. Two new flavones from Colebrookea oppositifolia. *Indian J. Chem.* **1981**, *20B*, 627.
(45) Reddy, R. V. N.; Reddy, B. A. K.; Gunasekar, D. A new acylated flavone glycoside from Colebrookea oppositifolia. *J. Asian Nat. Prod. Res.* **2009**, *11*, 183−186.
(46) Breitmaier, E.; Voelter, W. *Carbon-I3 NMR Spectroscopy*; VCH Publishers: New York, 1987.
(47) Buckingham, J.; Ranjit, V.; Munasinghe, N. *Dictionary of Flavonoids with CD-ROM*; CRC Press; Taylor and Francis, 2015; p 1199.
(48) Kobayashi, H.; Oguchi, H.; Takizawa, N.; Miyase, T.; Ueno, A.; Usmanghani, K.; Ahmad, M. New Phenylethanoid Glycosides from *Cistanchetubulosa*. *Chem. Pharm. Bull.* **1987**, *35*, 3309−3314.
(49) Zhang, J.; Huang, N.; Lu, J. C. Water-soluble phenolic compounds and their anti-HIV-1 activities from the leaves of Cyclocaryapaliurus. *J. Food Drug Anal.* **2010**, *18*, 398−404.
(50) Hayashi, K.; Hayashi, T.; Otsuka, H.; Takeda, Y. Antiviral activity of 5,6,7-trimethoxyflavone and its potentiation of the antiherpes activity of acyclovir. *J. Antimicrob. Chemother.* **1997**, *39*, 821−824.
(51) Saldanha, L.; Vilegas, W.; Dokkedal, A. Characterization of flavonoids and phenolic acids in MyrciabellaCambess.using FIA-ESI-IT-MS(n) and HPLC-PAD-ESI-IT-MS combined with NMR. *Molecules* **2013**, *18*, 8402−8416.
(52) Buckingham, J.; Ranjit, V.; Munasinghe, N. *Dictionary of Flavonoids with CD-ROM*; CRC Press; Taylor and Francis, 2015; p 1199.
(53) Tomas-Barberán, F. A.; Msonthi, J. D.; Hostettmann, K. Antifungal epicuticular methylated flavonoids from Helichrysum nitens. *Phytochemistry* **1998**, *27*, 753−755.
(54) Acton, Q. A. *Advances in Intestinal Mucosa Research and Application*; Technol Engineering, 2012, p 7148.
(55) Pegg, R. B.; Amarowicz, R.; Oszmiański, J. Confirming the chemical structure of antioxidative trihydroxy flavones from Scutellaria Baicalensis using modern spectroscopic methods. *Pol. J. Food Nutr. Sci.* **2005**, *55*, 43−50.
(56) Medzhitov, R. Origin and physiological roles of inflammation. *Nature* **2008**, *454*, 428.
(57) Satpathy, S. R.; Jala, V. R.; Bodduluri, S. R.; Krishnan, E.; Hegde, B.; Hoyle, G. W.; Fraig, M.; Luster, A. D.; Haribabu, B. Crystalline silica-induced leukotriene B 4-dependent inflammation promotes lung tumour growth. *Nat. Commun.* **2015**, *6*, 7064.
(58) Zhou, Y.; Wang, J.; Yang, W.; Qi, X.; Lan, L.; Luo, L.; Yin, Z. Bergapten prevents lipopolysaccharide-induced inflammation in RAW264. 7 cells through suppressing JAK/STAT activation and ROS production and increases the survival rate of mice after LPS challenge. *Int. Immunopharmacol.* **2017**, *48*, 159−168.
(59) Schottelius, A. J. G.; Mayo, M. W.; Sartor, R. B.; Baldwin, A. S. Interleukin-10 signaling blocks inhibitor of κB kinase activity and nuclear factor κB DNA binding. *J. Biol. Chem.* **1999**, *274*, 31868−31874.
(60) Medzhitov, R. Origin and physiological roles of inflammation. *Nature* **2008**, *454*, 428.
(61) Adewoyin, M.; Mohsin, S. M. N.; Arulselvan, P.; Zobir Hussein, M.; Fakurazi, S. Enhanced anti-inflammatory potential of cinnamate-zinc layered hydroxide in lipopolysaccharide-stimulated RAW 264.7 macrophages. *Drug Des., Dev. Ther.* **2015**, *9*, 2475−2484.
(62) Khajuria, V.; Gupta, S.; Sharma, N.; Kumar, A.; Lone, N. A.; Khullar, M.; Dutt, P.; Sharma, P. R.; Bhagat, A.; Ahmed, Z. Anti-inflammatory potential of hentriacontane in LPS stimulated RAW 264.7 cells and mice model. *Biomed. Pharmacother.* **2017**, *92*, 175−186.
(63) Cher, J. Z. B.; Akbar, M.; Kitson, S.; Crowe, L. A. N.; Garcia-Melchor, E.; Hannah, S. C.; McLean, M.; Fazzi, U. G.; Kerr, S. C.; Murrell, G. A. C.; Millar, N. L. Alarmins in frozen shoulder: a molecular association between inflammation and pain. *Am. J. Sports Med.* **2018**, *46*, 671−678.
(64) Bijlsma, J. W.; Jacobs, J. W. Glucocorticoid chronotherapy in rheumatoid arthritis. *Lancet* **2008**, *371*, 183−184.
(65) Kirwan, J.; Power, L. Glucocorticoids: action and new therapeutic insights in rheumatoid arthritis. *Curr. Opin. Rheumatol.* **2007**, *19*, 233−237.
(66) Liberman, A. C.; Budziñski, M. L.; Sokn, C.; Gobbini, R. P.; Steininger, A.; Arzt, E. Regulatory and mechanistic actions of glucocorticoids on T and inflammatory cells. *Front. Endocrinol.* **2018**, *9*, 235.

https://doi.org/10.1021/acsomega.1c01837
ACS Omega 2021, 6, 30241−30259

(67) Breitmaier, E.; Voelter, W. *Carbon-I3 NMR Spectroscopy*; VCH Publishers: New York, 1987.
(68) Chen, Y.; Lin, Y.; Li, Y.; Li, C. Total flavonoids of HedyotisdiffusaWilld inhibit inflammatory responses in LPS-activated macrophages via suppression of the NF-κB and MAPK signaling pathways. *Exp. Ther. Med.* **2016**, *11*, 1116−1122.
(69) Makarov, S. S. NF-κB as a therapeutic target in chronic inflammation: recent advances. *Mol. Med. Today* **2000**, *6*, 441−448.
(70) Li, N.; Xu, H.; Ou, Y.; Feng, Z.; Zhang, Q.; Zhu, Q.; Cai, Z. LPS-induced CXCR7 expression promotes gastric Cancer proliferation and migration via the TLR4/MD-2 pathway. *Diagn. Pathol.* **2019**, *14*, 3.
(71) Blander, J. M. The many ways tissue phagocytes respond to dying cells. *Immunol. Rev.* **2017**, *277*, 158−173.
(72) Necas, J.; Bartosikova, L. Carrageenan: a review. *Vet. Med.* **2013**, *58*, 187−205.
(73) Viji, V.; Helen, A. Inhibition of pro-inflammatory mediators: role of Bacopa monniera (L.) Wettst. *Inflammopharmacology* **2011**, *19*, 283−291.
(74) Smolinski, A. T.; Pestka, J. J. Modulation of lipopolysaccharide-induced proinflammatory cytokine production in-vitro and *in-vivo* by the herbal constituents apigenin (chamomile), ginsenoside Rb1 (ginseng) and parthenolide (feverfew). *Food Chem. Toxicol.* **2003**, *41*, 1381−1390.
(75) Khajuria, V.; Gupta, S.; Sharma, N.; Tiwari, H.; Bhardwaj, S.; Dutt, P.; Satti, N.; Nargotra, A.; Bhagat, A.; Ahmed, Z. Kaempferol-3-o-β-D-glucuronate exhibit potential anti-inflammatory effect in LPS stimulated RAW 264.7 cells and mice model. *Int. Immunopharmacol.* **2018**, *57*, 62−71.
(76) Love, S.; Mudasir, M. A.; Bhardwaj, S. C.; Singh, G.; Tasduq, S. A. Long-term administration of tacrolimus and everolimus prevents high cholesterol-high fructose-induced steatosis in C57BL/6J mice by inhibiting de-novo lipogenesis. *Oncotarget* **2017**, *8*, 113403−113417.
(77) Salonen, T.; Sareila, O.; Jalonen, U.; Kankaanranta, H.; Tuominen, R.; Moilanen, E. Inhibition of classical PKC isoenzymes downregulates STAT1 activation and iNOS expression in LPS treated murine J774 macrophages. *Br. J. Pharmacol.* **2006**, *147*, 790−799.
(78) Eräsalo, H.; Laavola, M.; Hämäläinen, M.; Leppänen, T.; Nieminen, R.; Moilanen, E. PI3K Inhibitors LY294002 and IC87114 Reduce Inflammation in Carrageenan Induced Paw Oedema and Down Regulate Inflammatory Gene Expression in Activated Macrophages. *Basic Clin. Pharmacol. Toxicol.* **2015**, *116*, 53−61.
(79) Bin-Hafeez, B.; Haque, R.; Parvez, S.; Pandey, S.; Sayeed, I.; Raisuddin, S. Immunomodulatory effects of fenugreek (Trigonella-foenumgraecum L.) extract in mice. *Int. Immunopharmacol.* **2003**, *3*, 257−265.
(80) Sahu, M. S.; Mali, P. Y.; Waikar, S. B.; Rangari, V. D. Evaluation of immunomodulatory potential of ethanolic extract of Roscoeaprocera rhizomes in mice. *J. Pharm. BioAllied Sci.* **2010**, *2*, 346.
(81) Coskun, O.; Yakan, B.; Oztas, E.; Sezen, S.; Gunaydin, A. A. Antioxidant and hepatoprotective activity of vitamin E and EGb 761 in experimental endotoxemic rats. *Turk. J. Med. Sci.* **2000**, *30*, 427−432.
(82) Bafna, A. R.; Mishra, S. H. Immunomodulatory activity of the methanol extract of the floral head of Sphaeranthus indicus Linn. *Ars Pharm.* **2004**, *45*, 281−291.

https://doi.org/10.1021/acsomega.1c01837
ACS Omega 2021, 6, 30241−30259